NATIONAL ADVISORY COMMITTEE FOR AERONAUTICS

TECHNICAL MEMORANDUM 1289

THE DEVELOPMENT OF A HOLLOW BLADE FOR EXHAUST GAS TURBINES

By H. Kohlmann

Translation of ZWB Untersuchungen und Mitteilungen Nr. 788, December 1943

Washington
December 1950

NATIONAL ADVISORY COMMITTEE FOR AERONAUTICS

TECHNICAL MEMORANDUM 1289

THE DEVELOPMENT OF A HOLLOW BLADE FOR EXHAUST GAS TURBINES*

By H. Kohlmann

SUMMARY

The high exhaust-gas temperatures and the high tip speeds at which the exhaust-gas turbines of aircraft engines are operated subject the turbine blades to extremely high stresses. Since these high stresses can no longer be controlled by solid blades, the use of hollow blades with internal cooling was indicated. In order to meet the high blade temperatures and the efforts toward a small number of blades, it was necessary to find new ways of forming the profiles, as well as manufacturing the blades.

The efficiency of suitable profile forms was explored in flow measurements on blade models in cascade arrangement, and the superiority of profiles with well-rounded leading edge over the heretofore usual constant-pressure profile was confirmed. The lift and drag coefficients from airfoil theory were introduced and the relationship between cascade theory and turbine theory was established by suitable definition of the cascade efficiency. According to the data obtained in the flow measurements, the turbine blading was laid out, different from the usual method, according to the cascade theory, and the conventional profiles were replaced by Joukousky profiles.

In order to gain an insight into the temperature conditions at the blades, some calculating methods were developed by which the temperature distribution along the blade shank and over the blade profiles is determined with respect to gas temperature, volume of cooling air, and operating conditions of the turbine. The theoretical results were confirmed by temperature measurements on blade cascades.

Since no experimental data on the manufacture of hollow blades were available, the development of blade forms had to proceed simultaneously with the development of blade production methods with due regard to the possibilities of mounting the blades in the turbine rotor. Manufacturing methods developed in collaboration with outside concerns made it possible to produce a seamless blade first of drilled-out solid material and later of sheet metal and tubing.

*"Die Entwicklung einer Hohlschaufel für Abgasturbinen bei BMW-München." Zentrale für wissenschaftliches Berichtswesen der Luftfahrtforschung des Generalluftzeugmeisters (ZWB), Berlin-Adlershof, Untersuchungen und Mitteilungen Nr. 788, December 1943.

The manufacturing methods of blades from sheet metal and tubing produced, theoretically, two blade forms, that is, the two versions of the box-root blades with wide and narrow root in circumferential direction. A large number of blade forms and possibilities of mounting can be developed from these two blade forms. The most beneficial of these forms cannot be decided forthwith at the present stage of exhaust-gas turbine progress. Since the development of the box-root blade had progressed farthest at the BMW München, (figs. 32 and 33)*, and since it was imperative to produce as quickly as possible a tested blade which was suitable for quantity production, this version was retained.

The first blades of the series were of solid material (figs. 23 and 24). Improvements in manufacturing methods reduced the cost of this hollow blade without machining of the blade root from about 10 marks to 0.50 mark for the box-root blade (fig. 31). Simultaneously with the reduction of the number of blades from 66 to 50, it was possible to reduce the weight of the blade, 50 grams for the solid blade, first to 32 grams and then further to 23 grams for the hollow blade. Herewith the loading of the wheel disk by the centrifugal forces of the blades at 320 meters per second tip speed, measured at the median blade disk D_m = 280 millimeters, could be lowered from more than 200 tons to about half, and hence a simple design of blade root and wheel disk could be obtained.

As proved by experiment, the blade with box root (figs. 32 and 33) is suitable at 800° C stagnation temperature for tip speeds, measured at the median disk, up to 350 meters per second, provided that the ratio of blade length to mean wheel diameter does not exceed the value 0.16. To the indicated stagnation temperature, there corresponds, depending upon the magnitude of the heat gradient transformed in the turbine nozzle, a gas temperature up to 950° C. The values are test-run figures obtained with blades of FCMD material from the Böhler Company. The test run with the material SAS 8 (FBD) containing nickel was made at 970° C gas temperature and 375 meters per second tip speed (measured at D_m = 280 mm). Blade failure occurred after 6 3/4 hours. The volume of cooling air in all tests amounted to 8 percent of the gas weight.

1. INTRODUCTION

Exhaust-gas turbines utilized for driving the superchargers of airplane engines at maximum pressure altitude must be operated at high tip speed if the supercharger dimensions are to be practicable at the high pressure head required. This results in high stresses in the turbine blades due to the centrifugal forces. In addition, there are the

*NACA editor's note: It is called to the attention of the reader that, because of illegibilities in the copies of all figures used in preparing this translation, absolute accuracy in the notations thereon could not be achieved. The copies of figures reproduced represent the best that were possible with the limitations thus imposed.

bending stresses due to the gas forces and the added stresses due to thermal stresses arising from the uneven heating of the blade by the hot exhaust gases. Since the exhaust gases enter the turbine without being cooled, the blade temperature (above 600° C) makes it the highest stressed part of the supercharger and so governs the permissible tip speed and in a large measure also the highest permissible exhaust-gas temperature at which the turbine can be operated.

In consequence, the development of the turbine blades required particular accuracy. As the exhaust-gas temperatures of aircraft engines range between around 800° and 1000° C and such high temperatures had not yet been utilized, the design of the blades called for entirely new methods. The blades had to be cooled during operation and the profile sections so designed that the temperature distribution over the profile cross section was as uniform as possible. When solid blades are used for the full-admission turbine, the question of cooling the blade root arises. After an investigation had proved this to be insufficient at high gas temperatures and high tip speeds, internal cooling was resorted to. The blades were designed hollow and cooling air passed through the hollow space. But even the manufacture of hollow blades lacked experimental data. Suitable manufacturing methods had to be developed first, and then the blade forms had to be adjusted to the manufacturing possibilities.

2. DEVELOPMENT OF SUITABLE BLADE PROFILES

The velocity diagram of the turbine specifies the deflection of the flow in the blade cascade, but does not define the profile shape. Up to the present, the usual procedure of constructing the blade profiles had been such that the blade back at entry and exit was straight. The direction of this straight line corresponded to the directions of the inflow and outflow velocity w_1 and w_2. The transition of the two directions into one another and the blade curvature were presented by circular arcs whose radii were again in relationship to the blade spacing. This design provided profiles with a rather pronounced leading edge; such profiles are very sensitive to changes of air flow direction, (for example, pressure from the back).

The flow pattern in potential flow for a cascade with such profiles is represented in figure 1. When the inflow velocity w_1 is known, the velocity can be computed from the square of the network in the field of flow, while Bernoulli's equation defines the pressure at every point of the flow. Figure 2 shows the pressure distribution on the profile circumference determined on the basis of the flow pattern plotted against the profile projected on the chord SS. When the end points of the pressures are joined, the line encloses an area. The contents of this

area are proportional to the force exerted on the profile in the projected direction. It was found that a pressure jump occurs on the profile in the area of the straight exit, which may result in a separation of the flow. By designing the back of the blade at the exit as a uniformly bent curve instead of a straight line, these pressure jumps can be avoided. Figure 2 shows further that the portion of the force at the suction side of the profile amounts to almost two-thirds of the total force, hence, the importance attached to the back of the blade in the design and manufacture of the profiles.

It is readily apparent that the construction of the blade profiles described in the foregoing does not altogether satisfy the requirements of the laws of flow. The velocity triangle of the turbine specifies the deflection, but does not define the profile form. On the other hand, the efficiency of the turbine is greatly influenced by the profile form of the blade. So, in order to be able to develop profile forms of suitable efficiency, it was necessary to gain an insight into the actual flow conditions existing in the blade cascade; hence the flow measurements on model blades in cascade arrangement. The principal object was to ascertain the profile forms for exhaust-gas turbines which, theoretically, appear to be suitable. The tests were made on a constant-pressure profile and a high-pressure profile with rounded leading edge (fig. 3).

In order to be able to make the measurements incontestable, enlarged wooden models of the profiles were made and mounted in cascades. The cascade length was kept constant throughout the tests. To vary the flow direction, the cascade was attached to obliquely cut off nozzles, the oblique cut being of constant length. The height of the nozzle was variable. These nozzles were built on to an air chamber with orifice adjustable according to height of nozzle. The tests were made with air forced into the tank by a blower. The setup is illustrated in figure 4. The measurements were made by the momentum method and checked from time to time by pressure measurements (fig. 3) on the profile and by direct-force measurements.

By the momentum method, the profile drag is computed from the change in momentum which the cascade experiences. Therefore, the velocity distribution aft of the cascade was determined by survey with a pitot tube, and the deflection diagram plotted with the average value of the stream velocity

$$\overline{w}_2 = \frac{\int w_2^2 \, dx}{\int w_2 \, dx}$$

and the inflow velocity w_1 constant over the nozzle section. The cascade, the deflection diagram, and the stress diagram are given in

diagrammatical representation in figure 5. The stress diagram was plotted with the aid of the deflection diagram. With m denoting the mass flowing between two streamlines at a distance t from each other, the component of the reaction force along the axis of the cascade is

$$x = m\left(w_{u_2} - w_{u_1}\right)$$

and that at right angle to the axis of the cascade is

$$y' = m\left(P_1 - P_2\right) = ht\,\frac{\rho}{2}\left(w_{u_2}{}^2 - w_{u_1}{}^2\right) + htp'$$

with

$$p' = P_K - P_{stagnation} = P_K - \left(P_2 + \gamma\,\frac{w_2{}^2}{2g}\right)$$

the pressure difference necessary to overcome the cascade drag.

The two components combined give the force R exerted by the flow on the profile. Decomposition of this force at right angles and parallel to w_∞ gives the lift A' and the drag W of the profile.

In airfoil theory and in blower design, it is customary to represent the lift and drag nondimensionally by the lift coefficient c_a and the drag coefficient c_w. It is conceivable that these values can be used for turbine cascades also. If the lift coefficient is defined by the equation $A' = c_a\,\frac{\rho}{2}\,w_\infty{}^2\,hl$ and the drag coefficient by $W = c_w\,\frac{\rho}{2}\,w_\infty{}^2\,hl$, the two values can be computed from the deflection diagram. If the lift coefficient is plotted against the drag coefficient with due allowance for the deflection (angle of inflow α), the characteristics of the profile are defined by these plots.

Figure 6 shows the two plots for the constant-pressure profile and the high-pressure profile. While the practical c_w-values on the constant-pressure profile are restricted to a narrow range of angles, and the drag increases considerably beyond this range, the high-pressure profile manifests only a slight increase in c_w over a wide range of angles. Moreover, the drag coefficients recorded on the high-pressure profile are considerably lower than on the constant-pressure profile.

The tie-in with the turbine theory is effected by introducing the cascade efficiency η. If the cascade efficiency is defined as

$$\eta = \frac{\text{energy downstream from the cascade}}{\text{energy upstream from the cascade}}$$

this value is identical with the conventional blade loss coefficient ψ^2 of the turbine theory.

Figure 7 represents these values plotted against the deflection $\frac{\beta_1 + \beta_2}{2}$. For the chosen spacing conditions, the flow angle β_2 remains constant independent of the inflow direction. The values shown in figures 6 and 7 were measured in the central section of the cascade.

These flow investigations indicated theoretically the superiority of the profile with rounded leading edge over the ordinary constant-pressure profile, and prompted the design of the profiles by the cascade theory. The circular-arc profile corresponding to the deflection diagram was constructed according to the rules of the cascade theory (reference 1) and a profile plotted with it as median line, thus affording a favorable channel form. In order to obtain geometrically feasible profile shapes, a Joukowsky profile was subsequently drawn around the circular-arc profile. The curvature parameter is fixed by the circular-arc profile, leaving only the choice of the thickness parameter arbitrary. The use of these profiles produced very beneficial channel forms, as indicated in figure 8.

To check the data obtained by the flow measurements on the model cascades, the characteristic curves of the turbine were compared with constant-pressure profiles and Joukowsky profiles. The number of turbine blades equipped with constant-pressure profiles amounted to 66, and those equipped with Joukowsky profiles, to 50 (fig. 9). The envelopes of the lines u = constant for both profile forms and the two lines $u = 195$ meters per second and $u = 276$ meters per second are represented. Here is brought out the greater unsusceptibility of the Joukowsky profile against changes in flow direction through the somewhat flatter aspect of the efficiency curves.

A further viewpoint for the development of the profile form was the temperature distribution in the profile cross section. Since a substantial temperature rise beyond the mean temperature in the blade cross section is restricted to the vicinity of the stagnation point, the effect of the curvature at the profile inlet (stagnation point) on the heat-transfer coefficient was investigated. The relationship between heat transfer and curvature radius in the stagnation point is represented in figure 10. It is seen that the heat transfer, and, hence, the temperature near the stagnation point, increases appreciably with decreasing curvature radius. Thus, an increase in the rounding of the leading edge, proved by the flow measurements to be advantageous, is in accord with the

attempts to obtain the most uniform temperature distribution possible over the profile cross section.

3. TEMPERATURE DISTRIBUTION AND STRESSES IN THE SHANK OF THE BLADE

To promote the utmost utilization of the energy of the exhaust gases, the gases enter the turbine without cooling, as result of which the turbine-blade temperature, termed the stagnation temperature ϑ_a, becomes very high. (This is the temperature a noncooled blade would assume.) The stagnation temperature can be computed by the formula

$$\vartheta_a = \vartheta_g - \frac{A}{2g} c_1^2 - 0.85 w_1^2$$

where ϑ_g is the gas temperature, c_1 the discharge velocity of the gas from the nozzle, and w_1 the relative velocity. The value 0.85 is an empirical value and denotes the efficiency of conversion of velocity into temperature. At 900° C gas temperature, the stagnation temperature ranges between 780° and 820° C, depending upon the magnitude of the heat difference converted in the nozzle, and the initial velocity. Thus it is seen that the blade temperature is still very high even with adequate cooling. On bearing in mind that the strength of the blade material is intimately related with the temperature, it follows that the preliminary calculation of a blade is predicated upon the knowledge of the temperature distribution in the blade shank; hence the development of calculating methods by means of which the temperature distribution along the shank of the blade with respect to the shape of the shank, the profile form, and the volume of cooling air can be computed (reference 2).

The procedure (fig. 11) is briefly as follows: Consider an element of the blade shank of height dx; there is a heat flow along the shank due to heat conduction and a heat flow at right angle to it through the blade from the gas side toward the cooling-air side. Computing the heat volumes Q_1 to Q_4 and forming the heat balance for the steady state by equating the heat volumes entering and leaving the blade element, one obtains a differential equation. After a suitable choice of the limiting conditions, the solution of this differential equation gives the temperature distribution along the blade shank. The formula for computing the maximum blade temperature and the temperature at any point of the shank is represented in figure 11. The heat-transfer coefficient α_i at the cooling-air side was calculated by the formulas for the heat transfer in

pipes. The heat-transfer coefficient α_a at the gas side can be computed in two ways: The blade is visualized as being replaced by a pipe at right angle to the flow direction, or as being replaced by a plate parallel to the flow direction. The two heat-transfer factors are not so very far apart and should approach the actual value very closely, when reckoning with the average value from these figures.

In order to avoid the somewhat tedious calculation of the heat-transfer factors, a formula was developed with which the ratio of the heat-transfer factors $\frac{\alpha_i}{\alpha_a}$ can be computed direct from known quantities, namely

$$\frac{\alpha_i}{\alpha_a} = 0.514\left(\frac{F \sin \beta}{F_K}\right)^{0.735}\left(\frac{d_a}{d_i}\right)^{0.265}\left(\frac{T_i}{T_a}\right)^{0.183} p^{0.735}$$

where

F = annular surface of nozzle

β = direction of corresponding velocity w_1

$F_K = f_K$ = area of cooling air duct

z = number of blades

$d_a = \frac{U_a}{\pi}$, U_a = outside circumference of blade

$d_i = \frac{4f_K}{U_i}$, U_i = circumference of blade duct

T_i = absolute temperature of cooling air

T_a = absolute stagnation temperature

p = volume of cooling air in percent of weight of the gas

In the calculation of the temperature distribution, the heat transfer over the blade shank and that over the profile cross section were assumed constant.

Similar considerations give the temperature distribution over the profile cross section, as exemplified in figure 12, for a hollow-blade profile. By means of this isothermal field, the stresses in the shank cross section, produced by the nonuniform temperature distribution, can be computed (reference 3).

These calculation methods were checked by temperature measurements on blades in segment arrangement (fig. 13). Thermocouples were attached at various points on the profile and over the height of the shank. To minimize the measuring errors, the wires of the thermocouples rested in grooves. The segments were mounted in a nozzle (fig. 14), and the temperature distribution along the shank and over the profile cross section was measured in relation to the volume of cooling air and the gas temperature. Similar temperature measurements were made at the wheel disk, with the aid of fuse plugs spaced at different diameters over the circumference of the disk. Appropriate choice of the fuse plugs insured the exact temperature of the disk. To lower the disk temperature, the two wheel chambers were ventilated. As indicated in figure 15, it requires very little cooling air to lower the disk temperature substantially. Increasing the volume of cooling air beyond 1.5 to 2 percent serves no useful purpose, since the temperature drop obtainable in the disk is very small. To lower the stresses due to the centrifugal forces, the blade shank was tapered. The effect of the taper on the stresses in the blade cross section is represented in figure 16. A taper of $\frac{f_1}{f_2} = 2$ lowers the stress in the cross sections of the shank by about 27 percent. This means that the maximum shank stress, for example, which at 320 meters per second tip speed and with cylindrical shank amounts to 26.5 kilograms per millimeter^2, is reduced to 19.1 kilograms per millimeter^2 by this taper.

When the temperature distribution along the blade and the shape of the blade shank is known, the permissible tip speed for the blade can be computed. On plotting the temperature distribution against the height of the blade, there corresponds to each temperature (fig. 17) a specific creep strength of the blade material. Hence a curve for the variation of the creep strength over the height of the blade can be plotted. If the shank stress due to the inherent centrifugal forces for various tip speeds is also plotted, one of these lines u = constant is tangent to the curve of the creep strength. The creep strength is reached first in the blade cross section related to the tangential point. The position of this point therefore characterizes the dangerous cross section of the blade, and the line u = constant, which is tangent to the creep strength, indicates the highest permissible tip speed. According to figure 17, the effect of heat conduction onto the blade root extends only up to about 10 millimeters in blade height. Since the curve u_{max} = constant is tangent to the creep-strength curve in the ascending branch, it follows that even a relatively small temperature drop in this area, such as is obtained by improved cooling of the blade root, for example, especially when the blades are short, produces an appreciable increase in the permissible tip speed. Figure 17 shows further that the maximum permissible tip speed for a specific cooling-air volume is not only dependent upon the maximum blade temperature but also on the temperature distribution along the blade and on the design of the blade

shank. To be able to use high gas temperatures in the turbine at high tip speeds, the maximum blade temperature must be kept at a minimum.

Since the maximum blade temperature is directly related to the stagnation temperature and is governed by the velocity conditions in the turbine, this maximum temperature can be taken into consideration during the design of the turbine. This is accomplished according to the stagnation-temperature formula by expending as large a portion of the heat gradient as possible in the nozzle. The lowest stagnation temperature is obtained with constant-pressure turbines.

A possible reduction in maximum blade temperature from the point of view of blade design and cooling is essentially limited to an increase in the heat transfer on the cooling-air by increasing the rate of the cooling. This can be accomplished by increasing the volume of the cooling air (fig. 18) or, for equal volume of cooling air, by a geometrically similar reduction of the profile dimensions combined with an increase in the number of blades (fig. 19).

If large blade dimensions are to be retained, the use of inserts inside the blade shank offers the possibility of raising the rate of the cooling air and thus of lowering the maximum blade temperature. The temperature distribution along the blade can also be influenced by suitable design of the insert. Figure 20 shows, by way of example, the installation of such an insert in a hollow blade by spot welding.

Figure 21 represents, by way of comparison, the mean temperature measured with and without this insert and the corresponding creep strength of the material SAS 8 and the permissible tip speed. Thus an increase of 20 meters per second in the permissible tip speed, measured at the median graduated circle of the blade, is obtainable by means of the insert.

In this manner, it was possible to reduce the shank stresses to such an extent that, at 800° C stagnation temperature, the turbine can be operated at 350 meters per second tip speed with 8 percent cooling air without the insert. The blade material consisted of material SAS 8 containing nickel supplied by the Böhler firm and nonrationed Cr-Mn steel At the present time, the blades are made exclusively of Böhler Cr-Mn steel FCMD, Ruhrsteel D712 and Krupp CHV-special (Cromadur).

4. ASPECTS FOR THE DEVELOPMENT OF BLADE MANUFACTURING METHODS AND THE ATTACHMENT OF THE BLADES IN THE ROTOR

One of the most important factors involved in the manufacture of the blade and the design of the blade root was that shank and root were

to form one unit. This automatically ruled out all solutions in which the shank and the root are manufactured separately so that the blade consisted of two parts, although such a solution seemed to present some advantages, as shown in figure 26. In view of the multiplicity of blades in a turbine, the question of mass production had to be taken into particular consideration in the development of manufacturing methods. It called for a method of producing the blades in the shortest and simplest possible manner with little material consumption, i.e., a minimum of machining; and simplicity of manufacturing ruled out everything but tubing or sheet metal as original material. The technological properties of the materials involved made the solution a step-by-step process. As pointed out earlier, only Cr-Mn or Cr-Ni austenite were dealt with here. These metals possess the property of becoming very brittle at cold working, so that for a long time it was impossible to produce thin-walled tubing. Even the bending and drawing tests made with these metals proved negative, at first.

The first blades had to be made from the solid material, the two halves being welded together. This method could soon be replaced by seamless blades obtained by pressing from a milled-out solid. These blades were then subsequently replaced by blades of sheet metal and tubing, respectively.

The possibility of manufacturing the blade shank and the root in one piece made for a uniform and comprehensive construction of blade and rotor and insured a simple assembly of the blades in the turbine rotor. The mode of mounting the blade root in the rotor was, aside from the conditions resulting from the root stress due to the centrifugal forces, again governed by inexpensive machining of the blade root and the condition of interchangeability. The best type of mounting proved to be the fir cone version represented in figure 24 and, for the blades made of sheet metal, the modified version shown in figure 32.

5. MANUFACTURE OF HOLLOW BLADE FROM SOLID MATERIAL AND MOUNTING OF BLADE IN THE ROTOR

As already stated, there were absolutely no experimental data available for the manufacture of hollow blades. From the thermal stresses in the blade, it was found that the shape of the cooling-air duct had to be fitted to the profile form. It therefore could not be designed in geometrical forms such as could be obtained by drilling, for example. Entirely new ways of manufacturing hollow blades were therefore indicated.

The first of the hollow blades used by the BMW were manufactured in two parts. Each half of the cooling-air duct was milled out from a

rectangular block (fig. 22); then the two pieces were welded together, and the blade profile machined out in the usual manner. This is an involved and, at the same time, costly method with considerable waste of material. Since the cooling duct had to be obtained by milling, it could be adapted only approximately to the profile form; thus it produced different wall thicknesses over the section of the profile. As a result the temperature distribution over the profile section became unfavorable and caused high heat stresses in operation. The welded seams came into zones of high stresses and frequently induced blade failure.

To promote a better temperature distribution, hence, improved stress conditions, as well as to simplify the manufacture of blades, attempts were made in 1939 to produce seamless blades by pressing from a milled-out body. In cooperation with the Leistritz Co., Nürnberg, it was possible to develop a suitable mass-production method. The manufacturing process is illustrated in figure 23. It shows the rough blank of heptagonal shape favorable for the root extrusion, and in form of bars obtained by rolling. The subsequent machining process consists of milling the shank and of a centric drilling operation in the manufacture of the cooling duct. The blank is swage-pressed into a blade at forging temperature. By inserting a core in the form of the finished cooling duct into the hole of the blank, it was possible to press the blade into finished size. The difficulties encountered, at first, when trying to extract the inserted core from the cooling duct, were overcome by the use of a suitable lubricant. The next step consisted in machining the blade root by milling the four sides, followed by machining the attachment grooves by a specially designed turning device (fig. 25). This device consisted of a disk provided with shoulders and previously machined grooves which served as template. The blades are clamped tight by placing two blades with a wedge pressed in between them between each two such shoulders. Accurate alinement of the blades in the turning device is insured by a stirrup at the shank tip. As is seen from figures 23 and 24, the blades are fastened in the rotor by the so-called fir-cone root. Since the centrifugal force of the blade is very great - over 2000 kilograms at maximum speed - the design of the grooves required painstaking care. They were constructed with a view to favorable stresses, while the strength calculations were supplemented by photoelastic studies.

This mode of attachment called for a split rotor design. However, this constitutes no disadvantage, since one-piece disks are more expensive to manufacture, as a result of the ducts required for cooling, than the two-piece disks, which can be designed as simple bodies of revolution. Besides, this mode of attachment insures a simple assembling of the blade in the rotor and a favorable passage of the cooling air for the blades. The cooling air can be conveyed directly through the hollow rotor shaft to the blades.

These blades were mass-produced for the turbine 801 and have proved themselves in more than 3000 hours of operation. The cost of the finished blade is 12 marks, or about half of that of the welded version. The weight of the rough blank is 350 grams, and that of the finished blade, 34 grams. Judging from this difference in weight, the manufacture of the blade requires considerable machining. It also explains the comparatively high cost of the blade. For these reasons, the blade could not be considered as the final solution, and further attempts to find less expensive methods were indicated.

One simplification in the blade manufacture was achieved by separation of blade shank and root (fig. 26). The shank was bent from heat-resistant contoured sheet metal and welded along the trailing edge. The profile of the sheet metal, that is, the point at the end of the shank, the cylindrical center piece, and the conical shank were produced by rolling before bending. The root piece was made from aircraft construction material 1610.5 and 1310.5 in one- and two-piece versions. On the one-piece version, the recess corresponding to the blade shank was stamped at forging temperature. On the two-piece version, the root piece was made from two rolled (steel) sections, welded together. The shank was then pushed into the recess of the root and the centrifugal forces taken up by the shoulder or collar provided at the end of the shank. The shoulder can be unloaded by providing a welded seam. This blade was less expensive and presented a saving in alloyed material, but its total weight remained the same.

A substantial weight reduction to about 26 grams was afforded by the version represented in figures 27 and 28. In this instance, the original material was a thick-walled tubing, rough-turned on the lathe, pressed and then machine-finished on the root. This blade, while meeting every strength requirement, was not put on a production basis, because it still was impossible to procure the correct tubing. It had to be milled from round stock which did not make for a much cheaper manufacture. Next, it was attempted to bend a sheet metal blade, but, since the shoulder at the blade root which serves to transfer the centrifugal forces onto the wheel disk had to be made comparatively wide, the thickness of the original sheet was so great that the rolling-out process of the sheet to its final size, which at the tip of the blade shank is only 0.4 millimeter, presented difficulties.

6. MANUFACTURE OF HOLLOW BLADE OF SHEET METAL

(BOX-ROOT BLADE)

It was found that a substantially simpler manufacture and hence a less expensive blade was contingent upon the development of a process

by which the original material could be shaped into the finished blade without machining. This is possible only when sheet metal or other suitable tubing can be used as original material, hence, attempts were made to bend the sheet metal blade. Bending and drawing tests on sheets of Cr-Mn steel were made. These tests, also carried out by the Leistritz Co., Nürnberg, indicated that these sheets did not lend themselves to much shaping in the cold state. Since shaping in the heated state was out of the question, it was attempted to facilitate the manufacture by suitable shaping of the blade. The blade was so constructed that the circumference at the root and at the shank was practically identical. This made it possible to restrict to a tolerable amount the stresses appearing during the shaping of the sheet into a blade, and so made it possible to manufacture the blade from sheet metal. The profile dictated by the taper of the blade shank and the shoulder at the transition from shank to root was produced by rolling prior to the bending operation. However, the wall thickness at the root and that at the shank could not differ too much from one another, else the rolling process would become excessive and the process more expensive again. The result was the blade with box root in the welded version, represented in figure 29. It shows the original material, the rolled steel section, and the manufacturing process. The blade is produced in five operations, namely: (1) rolling out of the sheet, (2) stamping of half of the blade in the top swage, (3) bending the remaining sheet around a core, (4) finish stamping of the blade in the bottom swage with core inserted, and (5) welding of the seam at the trailing edge.

This blade weighs only 23 grams and costs about 3.50 marks in the form shown in figure 29. This method was a great step forward as regards weight, material consumption, and cost of blade, but it was not particularly suitable for manufacture on a production basis. In addition, the welding had to be done by hand, since the seam is too short for automatic welding.

7. MANUFACTURE OF HOLLOW BLADE FROM TUBING

In the summer of 1943, the Württemberg Metal Manufacturing Co. in Geislingen finally succeeded in manufacturing tubing and therewith substantially simplifying the manufacturing method and reducing the price of the blade. The principal results are presented in figure 30. Out of a round semifinished flat a, whose thickness corresponds to the wall thickness of the blade root, a sleeve is produced by drawing, the bottom cut off, and the shoulder of the shank at the change-over to the root formed by drawing. The taper of the shank is also obtained by drawing. This rough blank, c, produced seamless by drawing, is pressed into a blade in the cold state after insertion of a core. The resultant blade forms are the same as when bent from sheet metal, but without

welding seam. This drawing process is eminently suitable for mass production, since the processes are quick and cheap, and the wear on the drawing tools very low. The cost of a finished blade, including material, is 0.40 to 0.50 mark, or only about 1/20 of that of the hollow blade made from solid metal. The weight of the blade, 23 grams, remained the same as that made of sheet metal.

8. FORMS OF BLADES WITH BOX ROOT

Figure 31 illustrates three versions of blades with box root. Versions a and b differ in width of root. On the blade with small root, the circumference at root and shank is identical, that is, the work piece has a continuous bore before the pressing operation. This obviates the filleting of the tube at the change-over from the root to shank, which makes this blade cheaper to manufacture than the blade with wide root. This blade also makes for small wheel heads. The two versions are characterized by the wide base at the root in circumferential direction. The blade roots are set side by side in the rotor so that the entire circumference of the rotor is covered from the inside. The bevel required on the contact surfaces is produced by milling, but it can also be obtained on the rough blank itself by an additional drawing operation. The bevel for 50 blades is 3° 07'.

The c version differs from a and b by its narrow base at the blade root. The blades c do not support one another after assembly in the rotor; whereas, the wide base in versions a and b guaranteed stable mounting of the blades in the rotor, the mounting of the blades in the rotor in the c version becomes difficult. The base of c being narrow, the blade must be set in deeper into the wheel, which soon becomes a problem of space. In that event, the roots of each pair of adjacent blades must be of different length such as is frequently done on solid blades with Laval root. But this makes the manufacture of the blade and the rotor more expensive again. Another disadvantage lies in the fact that, owing to the narrow inlet at the root, the cooling-air supply is no longer as favorable as with the wide-base blades.

From these shapes of the box-root blade, other shapes can be developed. Depending upon whether the side walls or the front walls of the box root are removed, it affords blades with root consisting of two lobes whose direction coincides with the circumferential direction or approximately with the direction of the rotor axis. All of these versions have the disadvantage, compared to the box root forming a supporting element as a whole, that the direction of the fiber is interrupted along the blade. This results in stress peaks, especially at the points where the lobes change over into the blade, which are apt to result in cracks and hence may lead to blade failure.

9. MOUNTING OF THE BOX-ROOT BLADES IN THE TURBINE ROTOR

The versions illustrated in figure 31 present two entirely different possibilities of fastening the blades in the turbine rotor. The blades with the wide base rest against one another at the root. As a result, the blades can: (1) be mounted by means of grooves between two halves of the wheel as with the fir-cone root, and (2) be mounted on the wheel from the outside and fastened. The second version with the narrow base indicated by c in figure 31 can be mounted in grooves which are provided at the circumference of the wheel disk in approximately axial direction.

To mount the blade with the wide base in a split turbine rotor, the attachment in grooves similar to those for the fir-cone root is advantageous. Since the weight of this blade is only about two-thirds of that of the solid blade, the size of the grooves can be kept smaller and also be made rectangular which presents less difficulties in the milling of these small rectangular grooves. It is even possible to mill several grooves at once with a forming tool. Figures 32 and 33 represent a version of such blade attachment with three grooves. Recent endurance tests at 900° C gas temperature and 325 meters per second tip speed, measured at the median blade disk portion with blades of Cr-Mn steel FCMD, indicated that the stresses developed can be just as safely controlled by two grooves. The grooves in the blade root can be turned on the lathe by means of a special device (fig. 25), or else milled out, which should be of particular advantage for mass production.

Figures 32 and 33 further show a simplified version of the turbine rotor. The disks, which thus far were provided with ribs on the inside as ducts for the cooling air, are now smooth (fig. 34). The hollow space formed by the two disks, and through which the cool air passes, is provided with radial feed grooves instead of the ribs. The radial feed grooves, pressed from sheet metal and centered in the two disks, obviate the expensive milling operation at the wheel disks; in this version the disk and the shaft, located on the side of the turbine shaft, which up to then were forged from one piece, are separately rough-cut and then electrically butt-welded and finished on the machine. This resulted in a further substantial reduction of the rotor production cost.

The two wheel disks (rotor and rotor cover) are attached by bolts which at the same time serve for taking up axial pressures introduced by the centrifugal forces of the blade and the heat expansion of the blade root.

This version of turbine rotor and blade attachment has proved very satisfactory in service. After an exhaustive examination of other attachment possibilities (to be discussed later), this version was put on a production basis and superseded that shown in figure 24.

A further possibility, which was not followed through, however, is the version with wire rings, shown in figure 35. The semicircular grooves of identical diameter milled in the blade roots and wheel disks face each other after assembly and form a circular annular groove. Wire rings inserted in these grooves serve to transfer the centrifugal forces of the blade to the wheel. The advantage of this type of mounting lies in the simple manufacture and particularly in the fact that the round shape of the grooves reduces the notch effect in the blade root and wheel rim to a minimum. But the circular wire introduces axial components of the centrifugal forces with a correspondingly high stress in the bolts on the wheel disk.

Two examples of the possibility of mounting the blades at the turbine rotor from the outside are given in figures 36 and 37. The grooves in the circumference of the rotor are so milled out that the tenons remaining between the grooves fit into the cavity of the box root. The blades are pushed over these tenons and then welded together (fig. 36) or joined mechanically, such as by means of a ring, for example. (See fig. 37.) The drawback here lies in the fact that the centrifugal forces of the blades must be taken up by these tenons, the dimensions of which are limited by the size of the box root. In the version shown in figure 36, the blade root has radially milled grooves into which the welding seams are placed. The radial arrangement insures a favorable stress distribution in the blade root. By suitably designed blade root, this version can be applied up to the highest tip speeds. A model wheel was manufactured and tested, but the solution was not followed through because a satisfactory weld of the austenitic blade material with that of the wheel disk introduced difficulties, and the application of welding made the interchangeability of blades impossible.

A particularly simple attachment of this kind is obtained when the built-up weld is replaced by spot welding. Provided that the bevel necessary on the lateral contact surfaces at the root was already effected on the rough blank, the blade can be mounted on the wheel as it comes from the press without any further machining. This solution was also abandoned, since the uncertainty inherent in the nature of spot welding gave rise to misgivings.

The version shown in figure 37 has the fundamental drawback that the direction of the fibers in the blade root is interrupted, aside from the fact that the highly stressed tenons at the rotor circumference are weakened further by the milling of the groove for the ring. This design is practical only for low stress.

In these and in the subsequently discussed versions the wheel disk could be produced in one piece, but this possibility was not taken advantage of because the two-piece rotor manufacture is less expensive in mass production. The attachment bolts in the wheel disk, however, could be omitted in most cases and rivets substituted.

The possibilities of mounting the blade with small box root in axial grooves at the wheel circumference are represented in figures 38 and 39. In figure 38, the blades are set in simple grooves and welded to the wheel disk. The advantages are simple manufacture of the grooves in the turbine rotor and the absence of machining at the blade root. On the other hand, the disadvantages accompanying welding must be taken into the bargain.

In figure 39, the centrifugal forces of the blades are taken up by the holding strip provided at the root of the blade. In the example denoted by a, these strips were formed by beading of sheet metal lobes which protrude over the box root. In the version denoted by b, these strips are welded to the root. The disadvantage here lies in the difficulties involved in the manufacture of the grooves at the rotor circumference. Besides, the webs at the rotor circumference which must take up the centrifugal forces of the blades as well as those of the heads at the end of the webs intended to transmit stresses and to serve as covering of the rotor circumference are subjected to extremely high stresses so that, at high tip speeds, the blade roots must be relieved by being given uneven lengths. These solutions were discarded.

From the versions of box roots presented in figure 31, further root shapes can be developed. Removing the front walls of the box root leaves a blade with root consisting of two lobes approximately coincident with the direction of the rotor axis. The blades are mounted in the rotor by pushing the blade with its lobes into grooves milled in the rotor circumference, each groove containing a lobe of two contiguous blades (fig. 40). This makes the process a little more complicated, but the number of grooves is restricted to a minimum and the blades insure a complete covering of the wheel circumference. Welding can be resorted to again, the seams being placed radially along the grooves. Placing the seams in circumferential direction has the added advantage that automatic welding machines can be utilized.

When welding is to be avoided, the lobes must be strengthened toward the bottom so that the blades can be held in suitable grooves of the wheel disk as exemplified in figure 41. There are several ways of strengthening the lobes. In the example of figure 42, the design of the lobe root was governed by the manufacture of the grooves in the wheel disk. The lobes were so designed that the reinforcement on the lobes of two contiguous blades which rest in one groove form a circle. This facilitates the drilling and milling of the grooves in the rotor.

The manufacture of such blades presents no difficulty. They can be formed from sheet metal, the reinforcement at the lobe tips being effected by rolling.

The second possibility in which the side walls of the box root are removed gives a blade with root formed by two lobes in circumferential direction, hence a blade like a rim-straddling bucket. The blades can be fastened to the wheel disk by pins or by built-up or spot welds. The advantage lies in the low cost, since no grooves are required on the rotor circumference.

Similar modifications can be developed from the box-root blade with narrow base. In this instance, the most diversified shapes of blades can be formed by combining the two ends of the lobes, the cooling air entering the blade from the sides. The blades can be assembled in various ways. But at the BMW in München, these possibilities could not be explored further, since each new blade design required considerable time before reaching the stage of quantity production and the BMW was charged with producing a blade ready for quantity production within the shortest possible time.

Translated by J. Vanier
National Advisory Committee
for Aeronautics

REFERENCES

1. Weinig, F.: Die Strömung um die Schaufeln von Turbomaschinen. Leipzig 1935 I.A.Bahrth.

2. Müller, A.: Die Innenkühlung bei Schaufeln von Abgasturbinen. ZWB Forschungsbericht Nr. 1386, 1941.

3. Pollmann, E.: Temperaturen und Beanspruchungen an Hohlschaufeln für Gasturbinen. ZWB Forschungsbericht Nr. 1879, 1943. (Available as NACA TM 1183.)

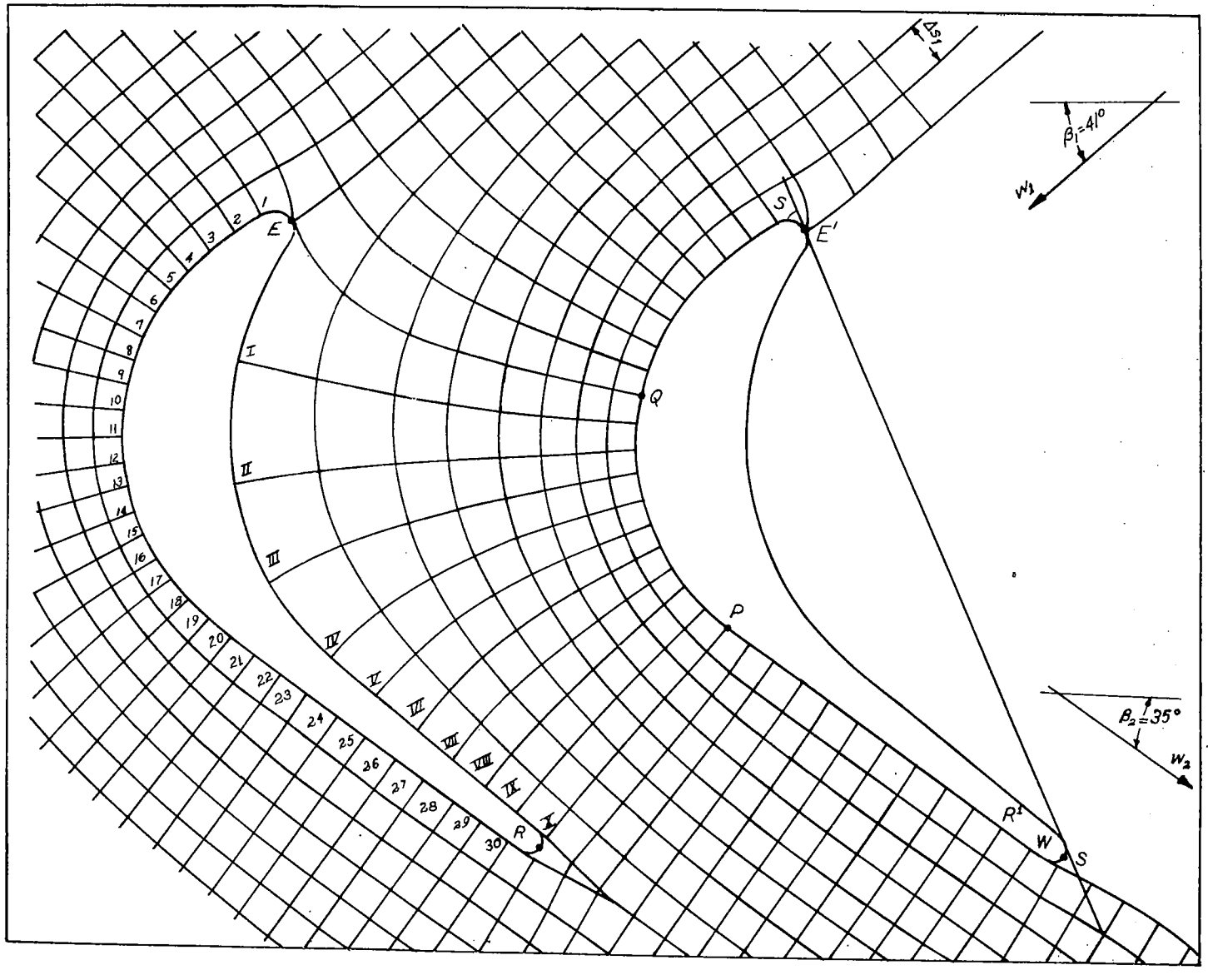

Figure 1.- Potential flow at the blades in cascades.

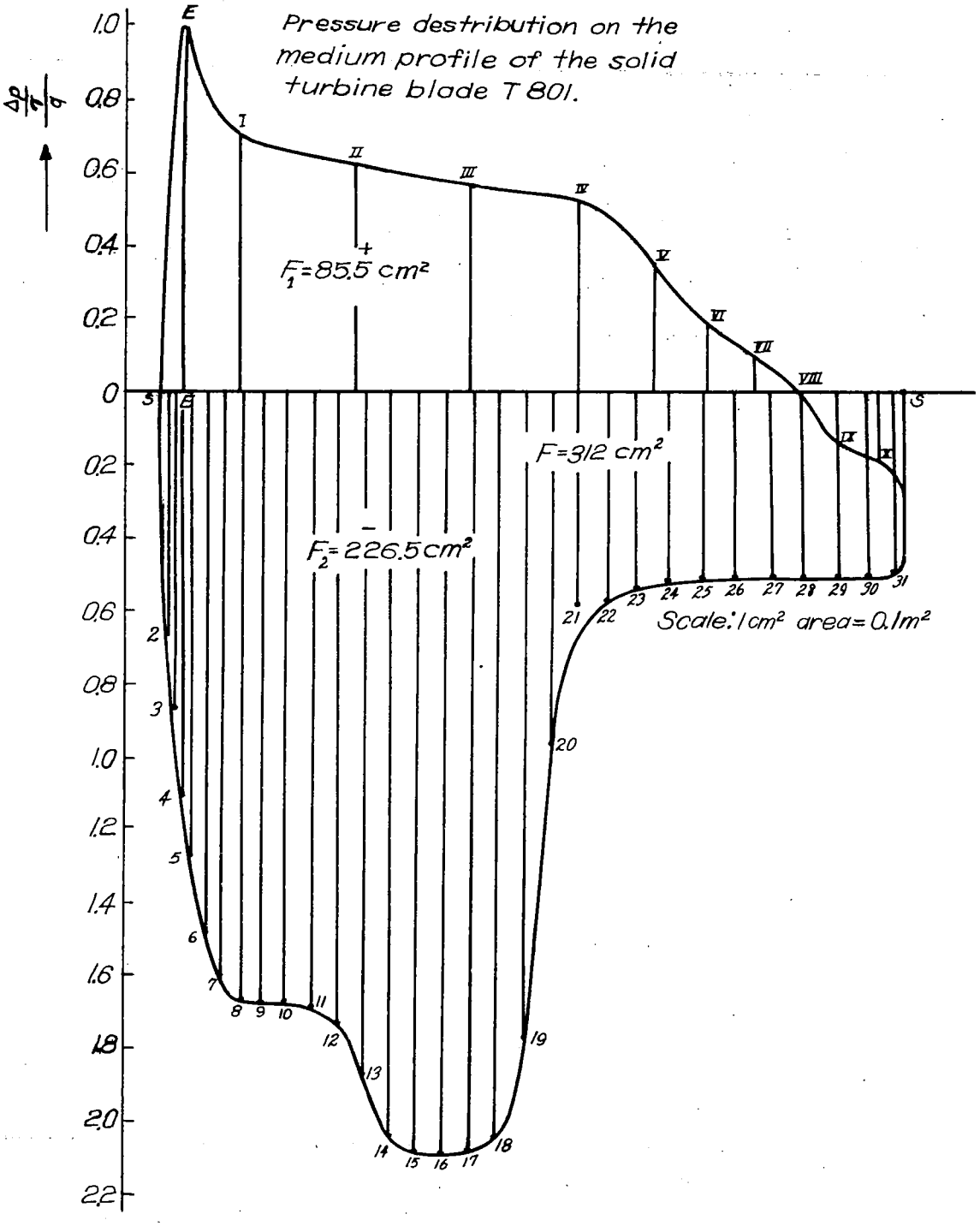

Figure 2.- Pressure distribution at the profile in cascades - potential flows.

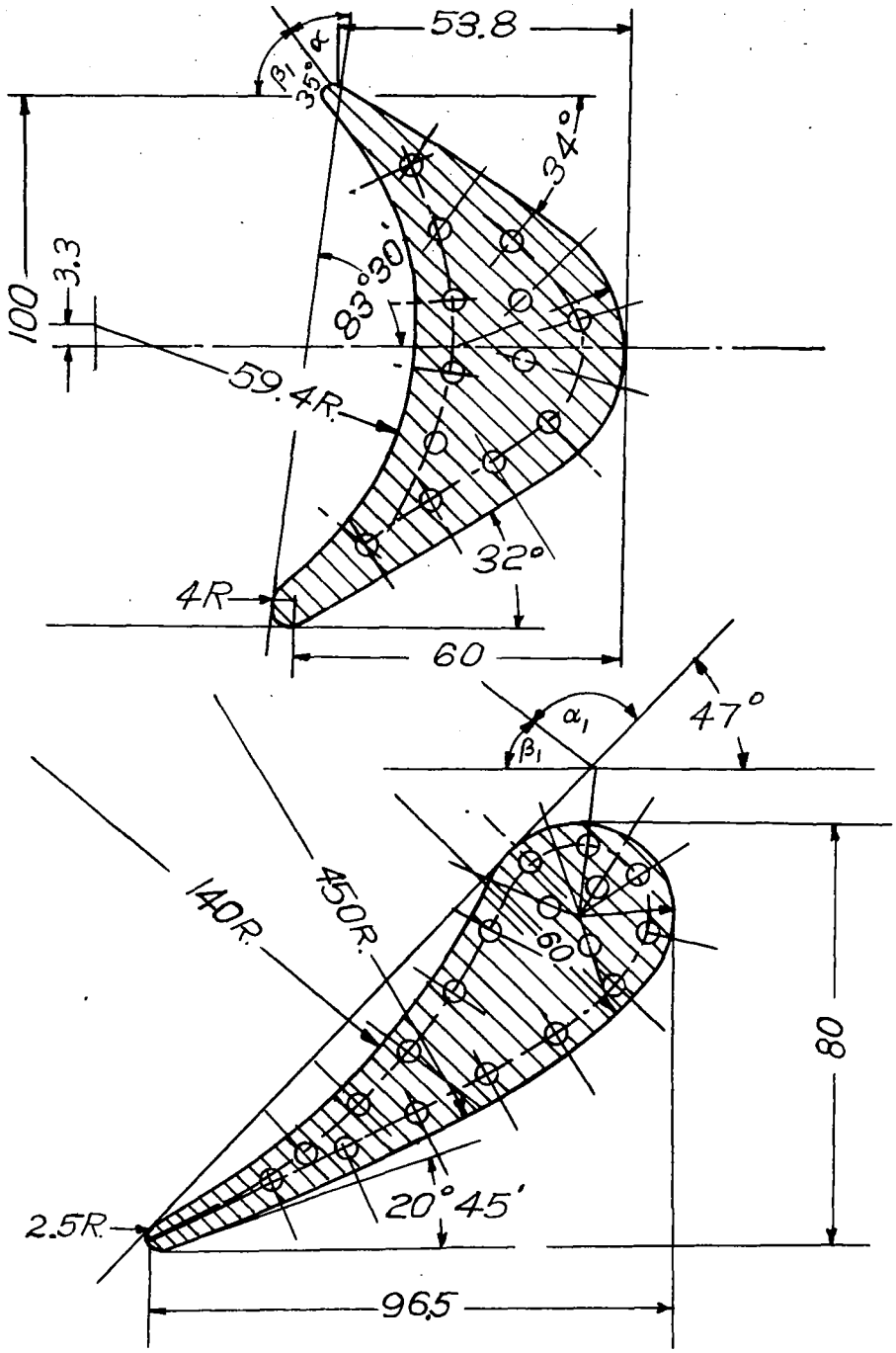

Figure 3.- Blade profiles and arrangement of pressure-recording stations.

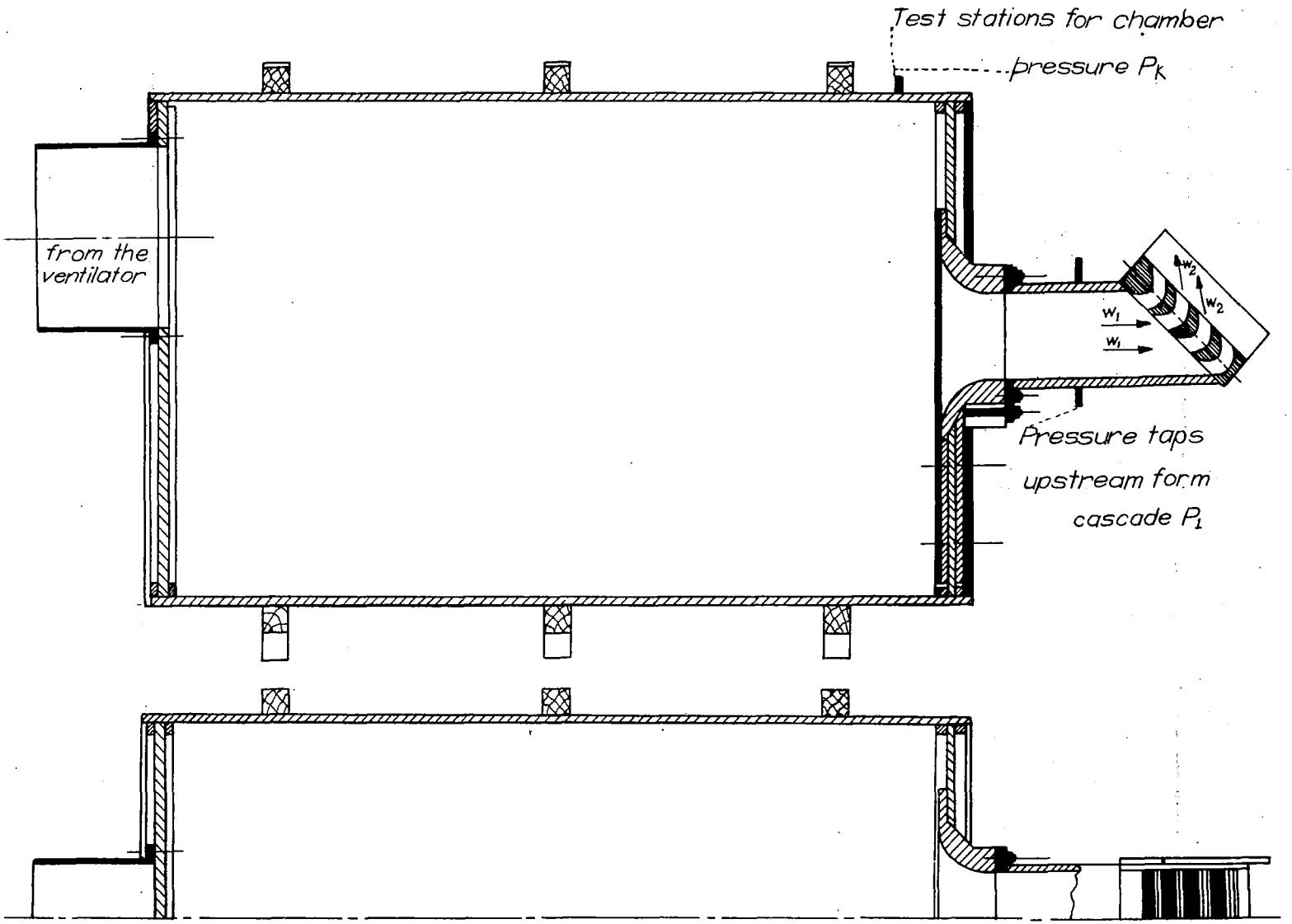

Figure 4.- Experimental setup.

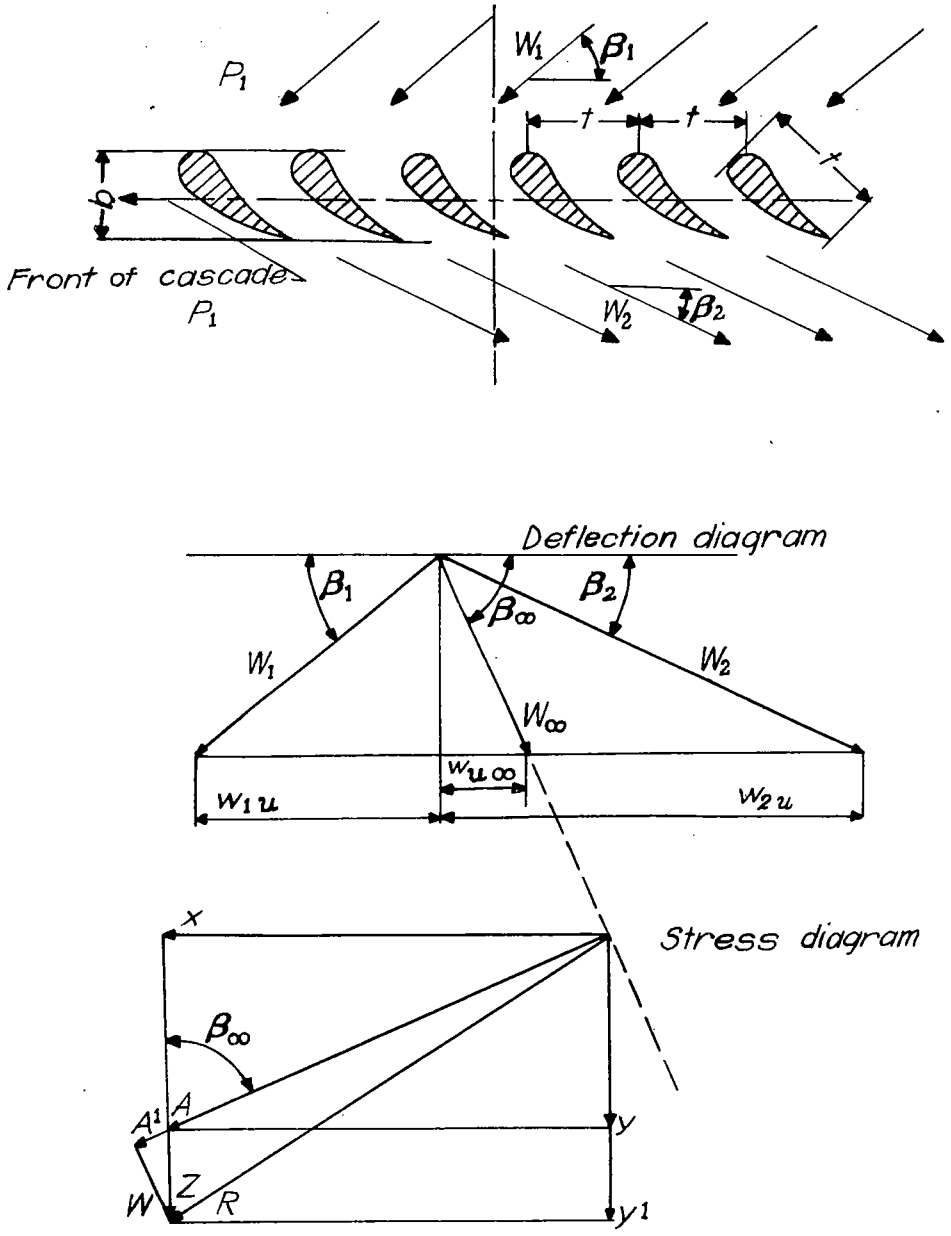

Figure 5.- Forces and velocities at the profile in cascade arrangement.

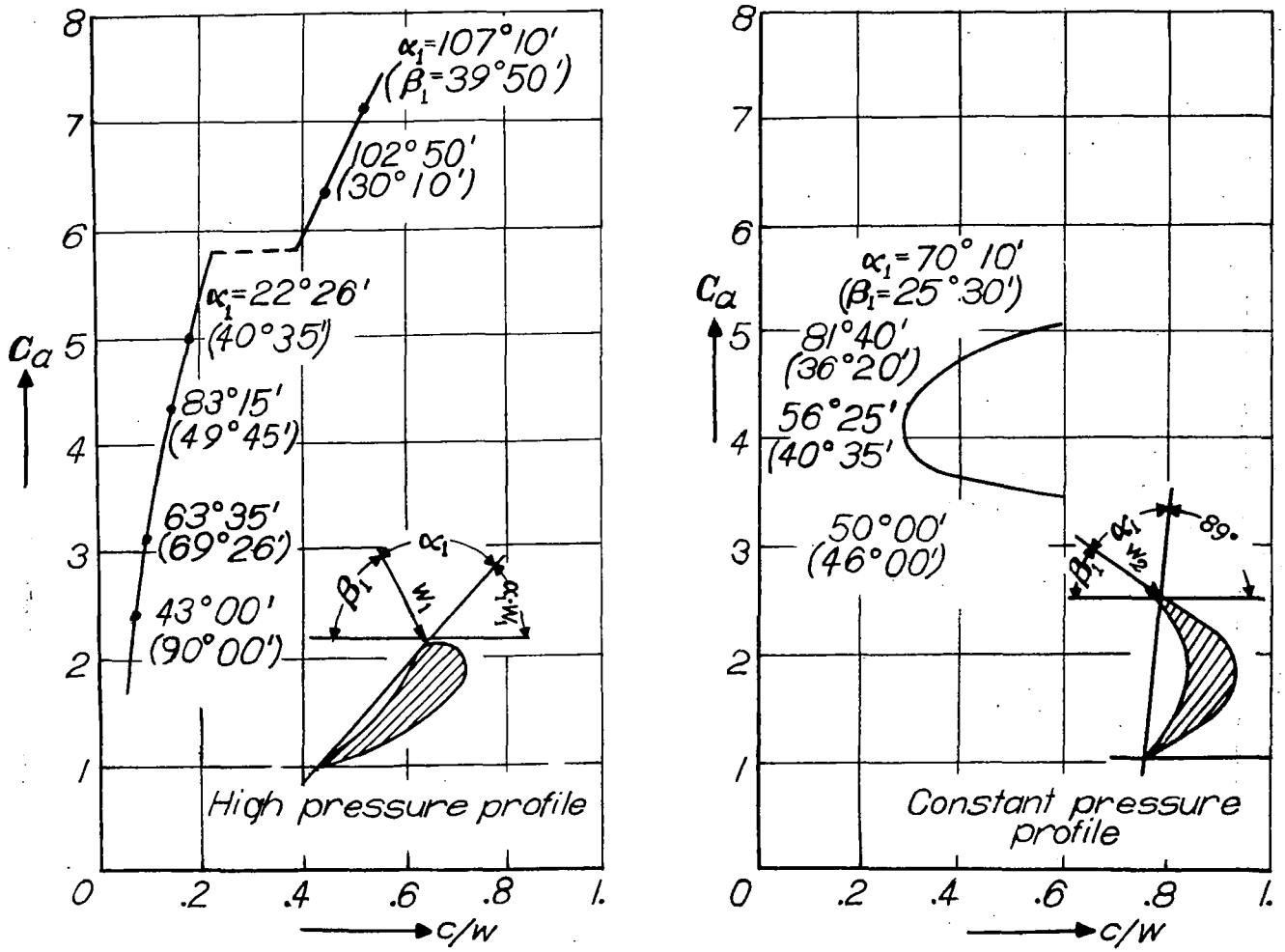

Figure 6.- Polars of the plotted profiles obtained by measurements on model cascades.

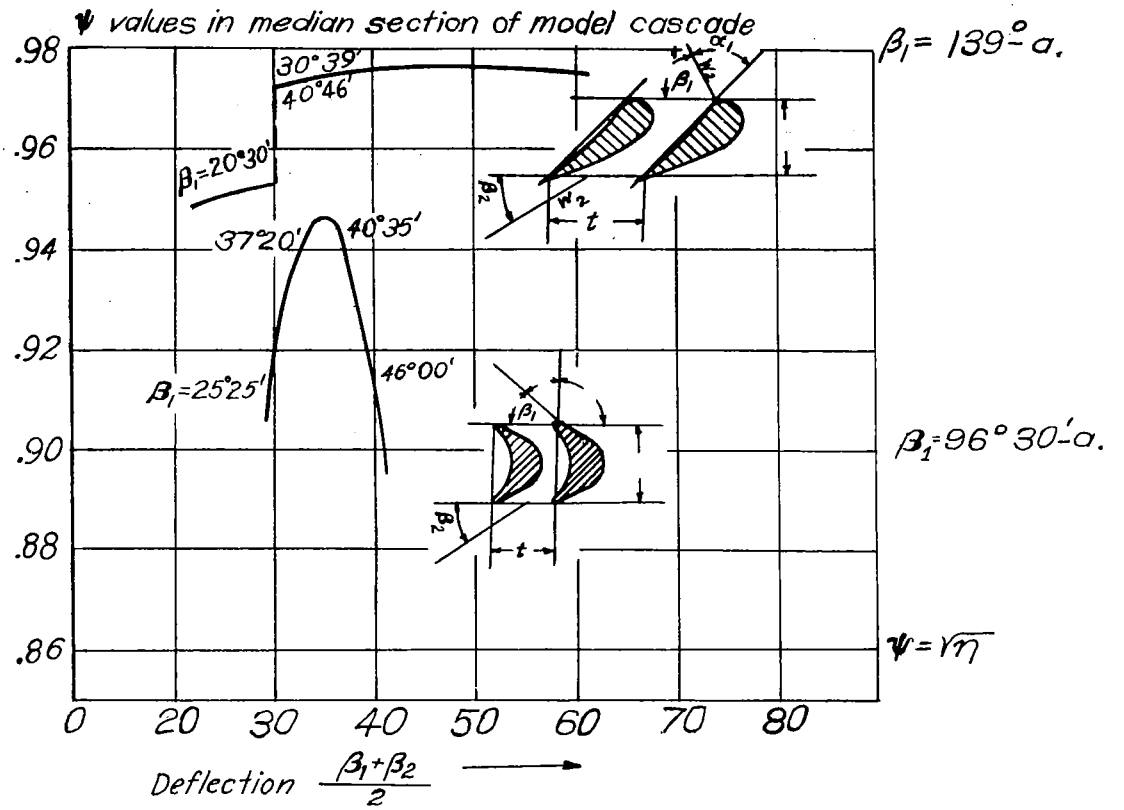

Figure 7.- Values of the plotted profiles obtained by measurements on model cascades.

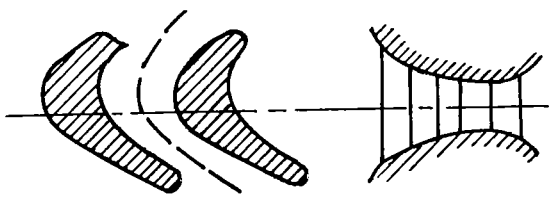

Constant pressure profile.

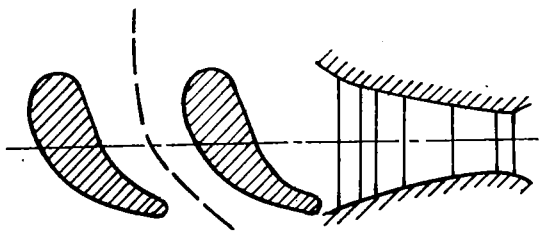

High pressure profile (Joukowsky profile).

Figure 8.- Channel form for constant-pressure and Joukowsky profiles.

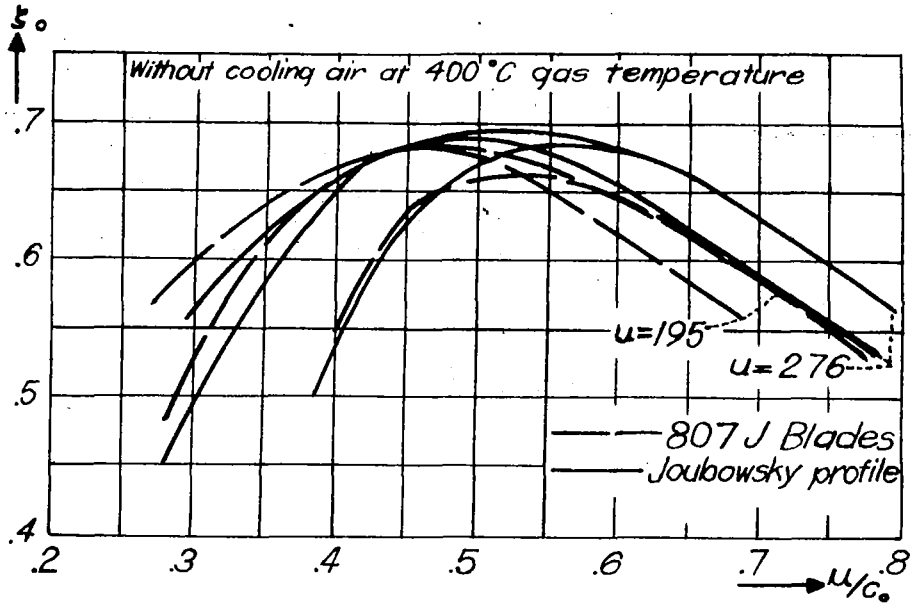

Figure 9.- Without cooling air at 400° C gas temperature.

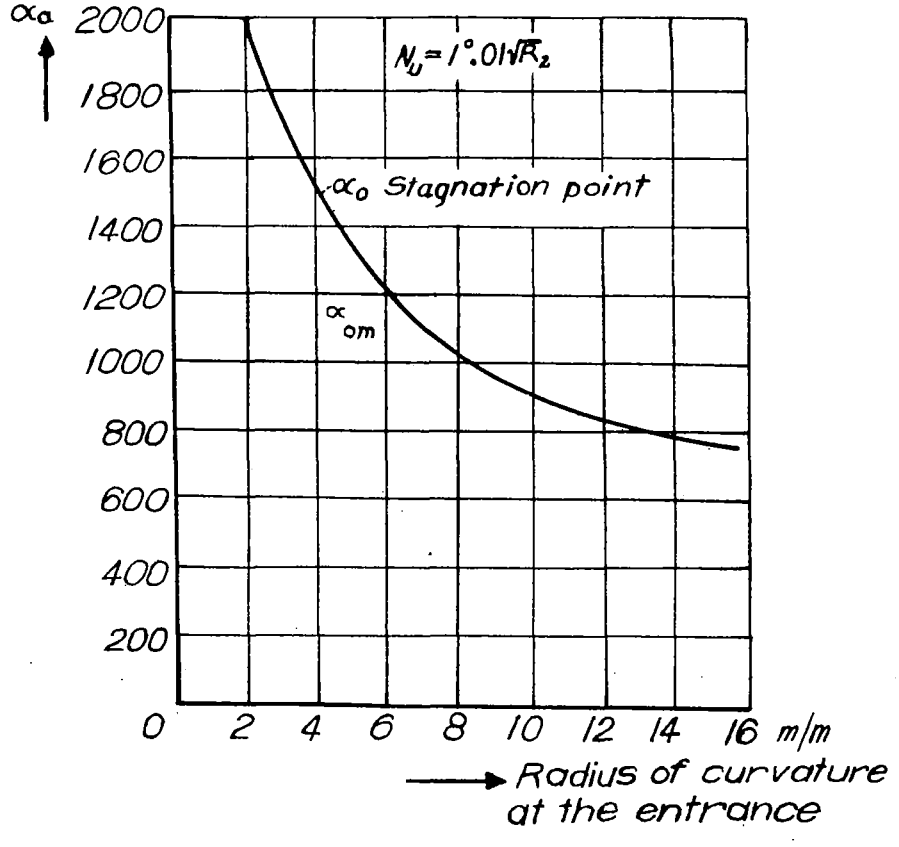

Figure 10.- Heat transfer and radius of curvature at the stagnation point.

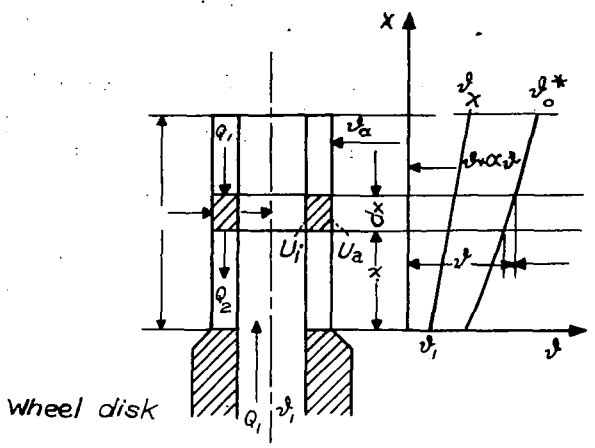

Figure 11.- Maximum blade temperature: $\vartheta_o^* \frac{\vartheta_2 + \alpha_i/\alpha_a \cdot U_i/U_a \vartheta_i}{1 + \alpha_i/\alpha_a \cdot U_i/U_a}$.

Blade temperature at point x: $\vartheta_x = \vartheta_o^* - \left(\vartheta_2^* - \vartheta_1^*\right) e^{-\beta k}$;

$\beta = \sqrt{\beta_a^2 - \beta_i^2}$; $\beta_a^2 = \frac{\alpha_a U_a}{\lambda f}$; $\beta_i^2 = \frac{\alpha_i U_i}{\lambda f}$.

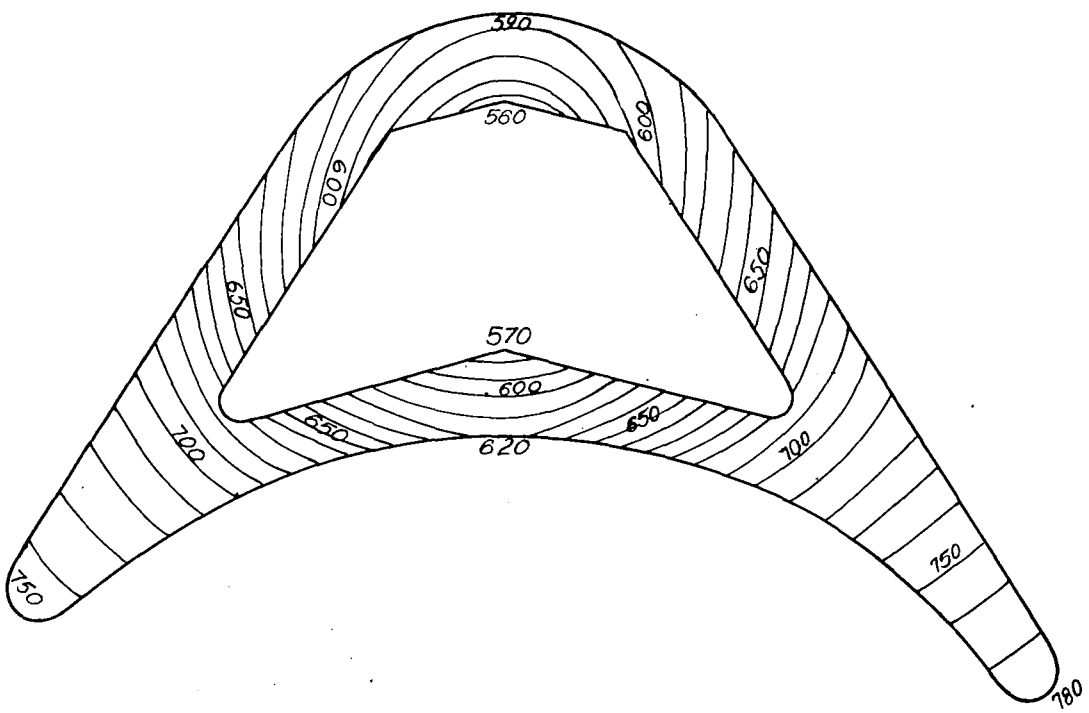

Figure 12.- Temperature distribution at blade cross section.

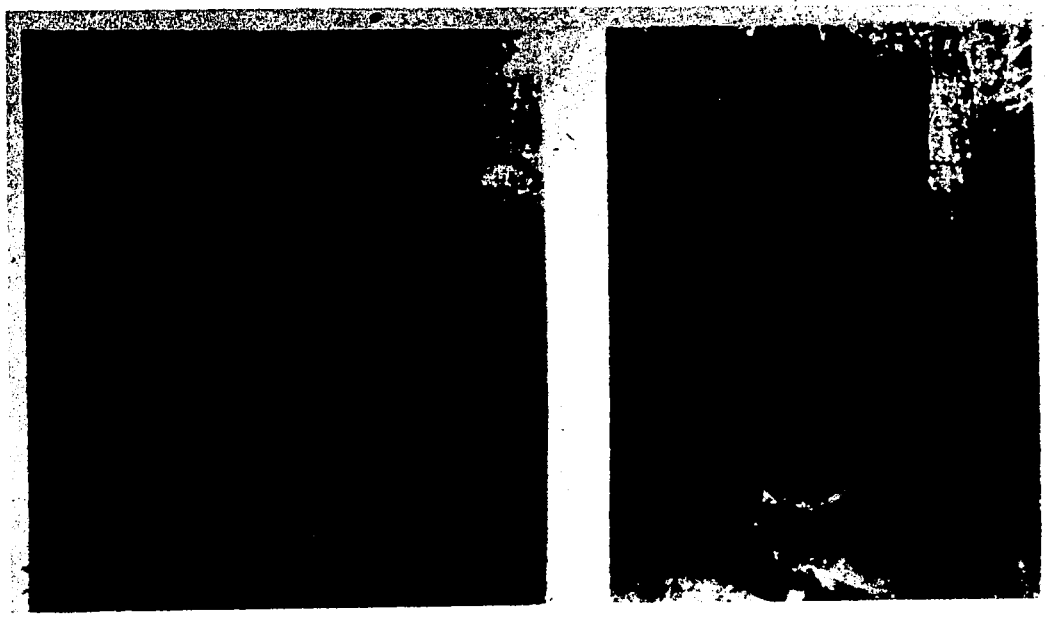

Figure 13.- Temperature measurement on blades in segment arrangement.

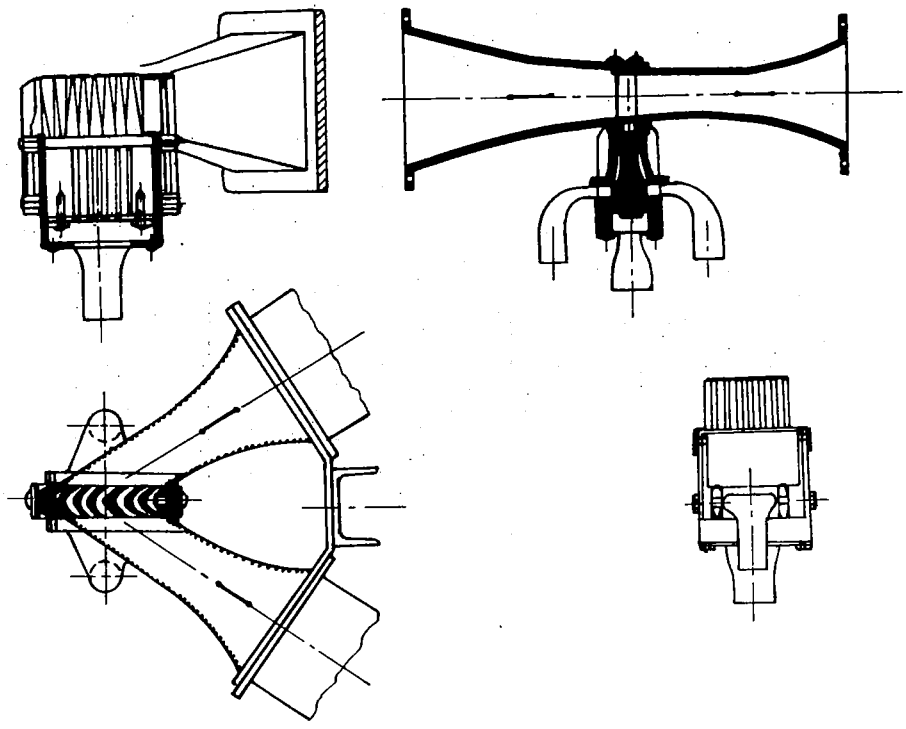

Figure 14.- Blade-temperature-measuring device.

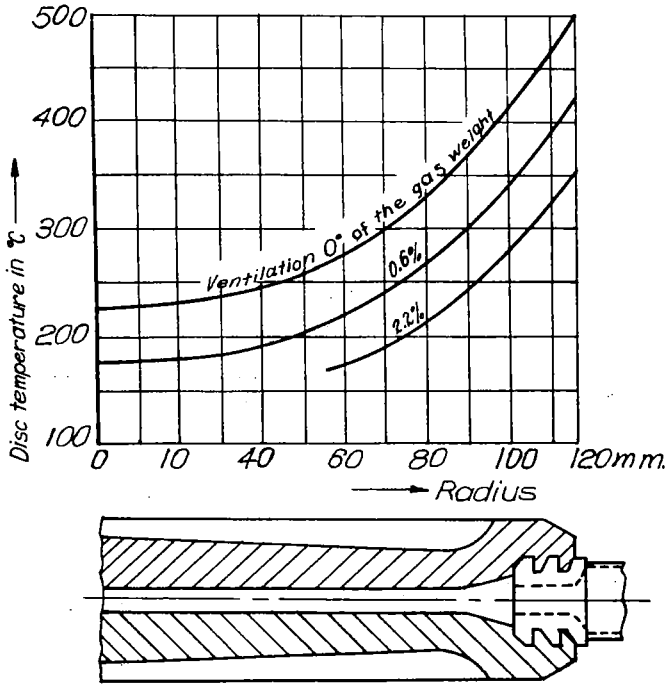

Figure 15.- Temperature of cooling air in shaft: 100° C; weight of cooling air: 10 percent of gas weight; gas temperature before nozzle: 750° C.

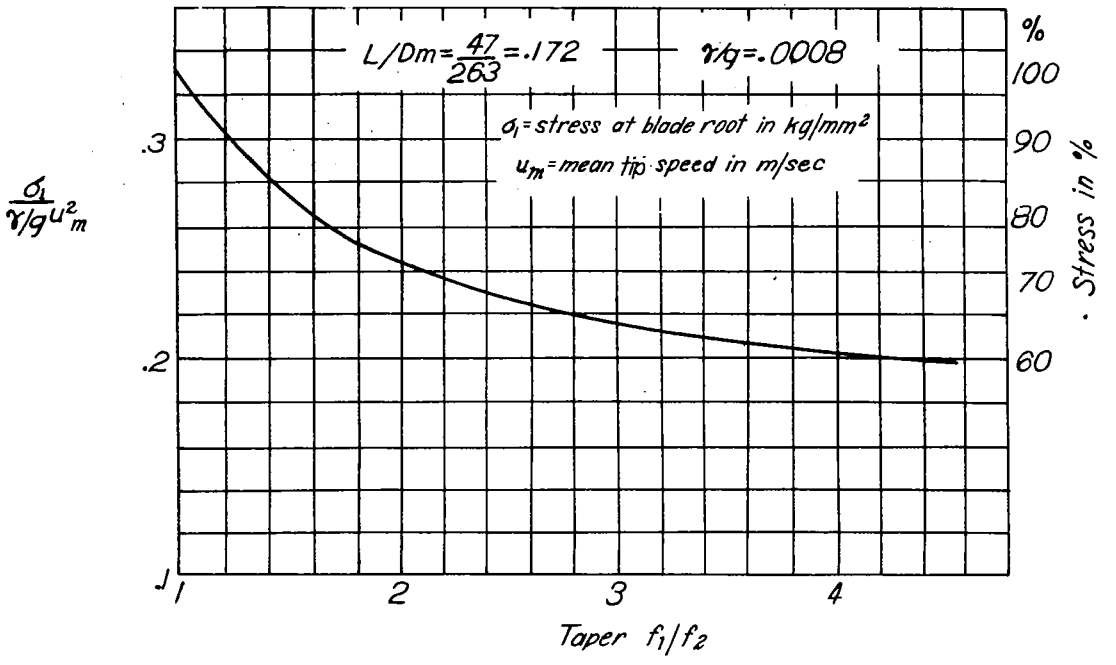

Figure 16.- Effect of taper on centrifugal stress of blade.

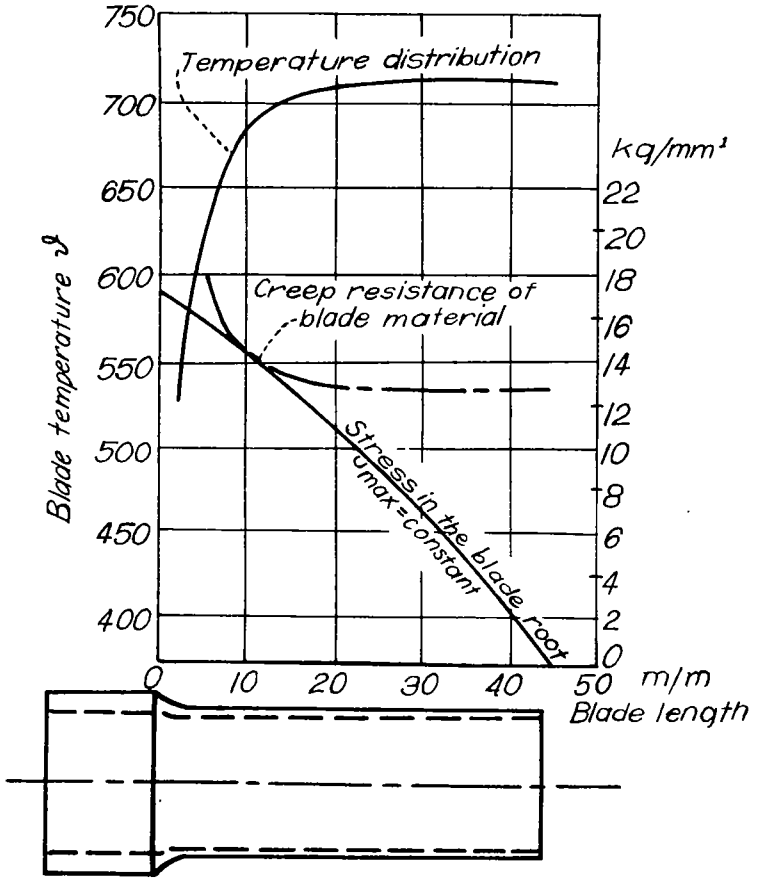

Figure 17.

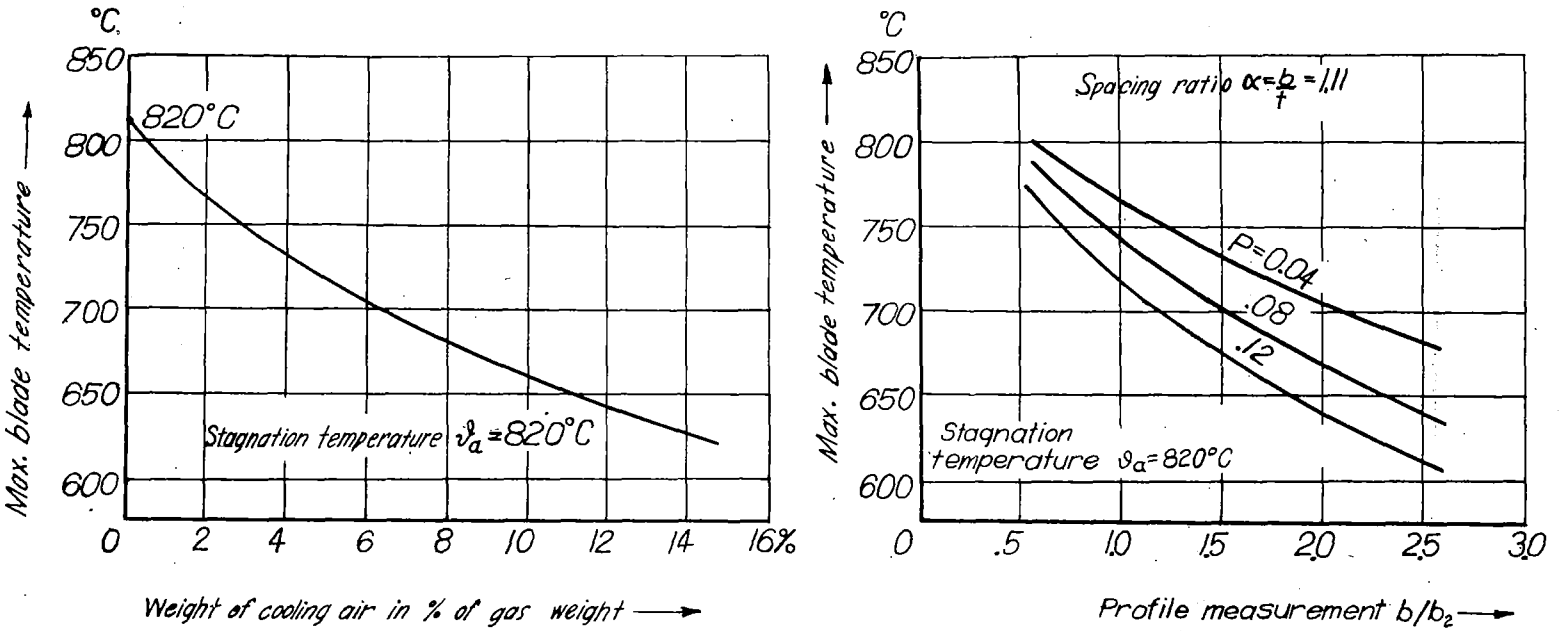

Figures 18 and 19.- Blade temperature plotted against volume of cooling air and profile dimensions of the blade with Joukowsky profile.

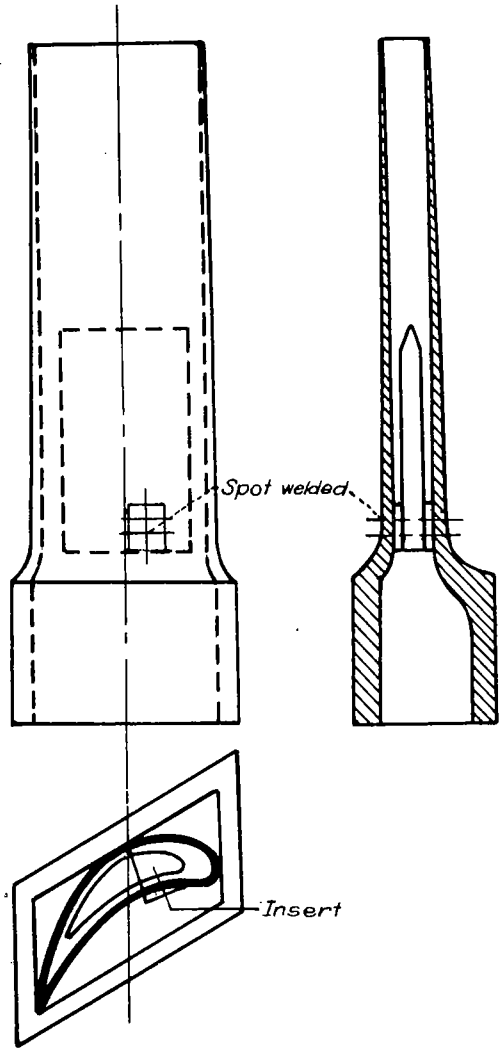

Figure 20.- Example of installation of insert in hollow blade.

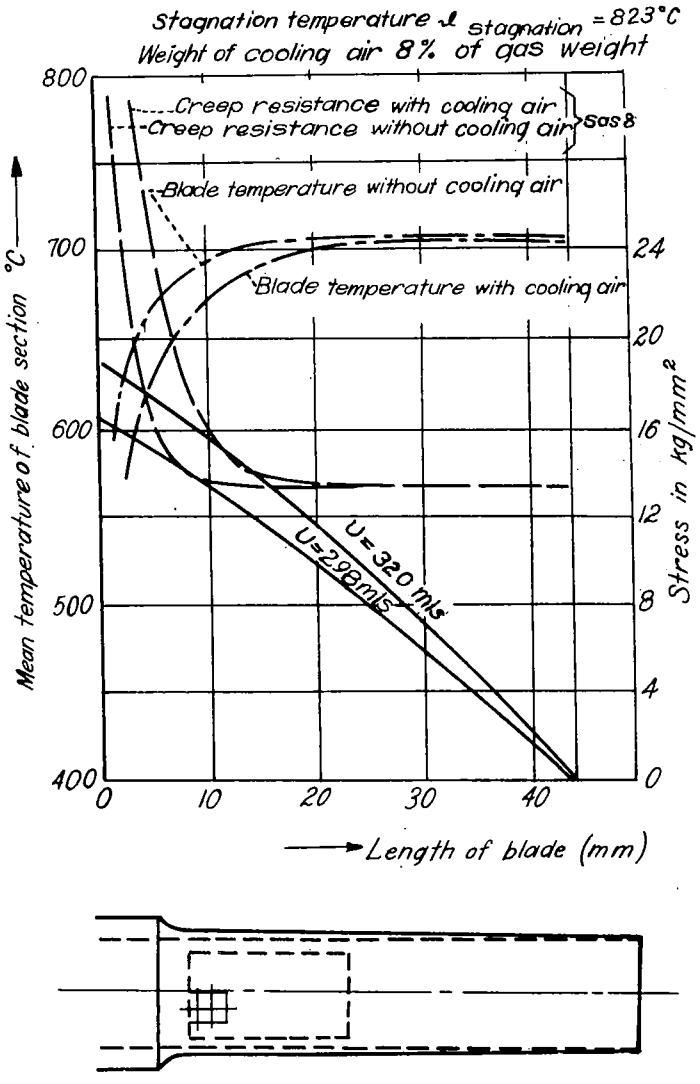

Figure 21.- Temperature distribution and permissible stress.

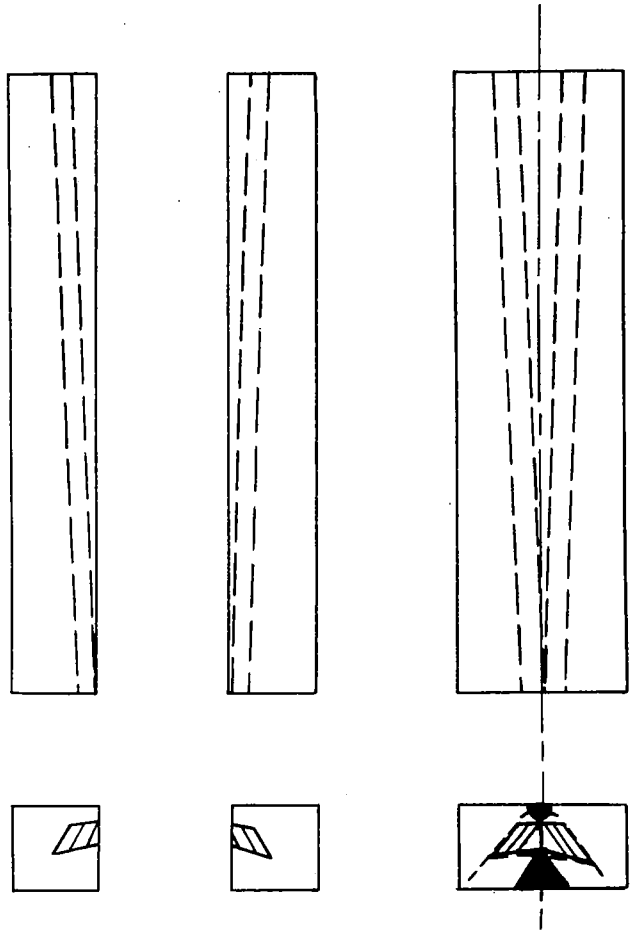

Figure 22.- First version of BMW hollow blade.

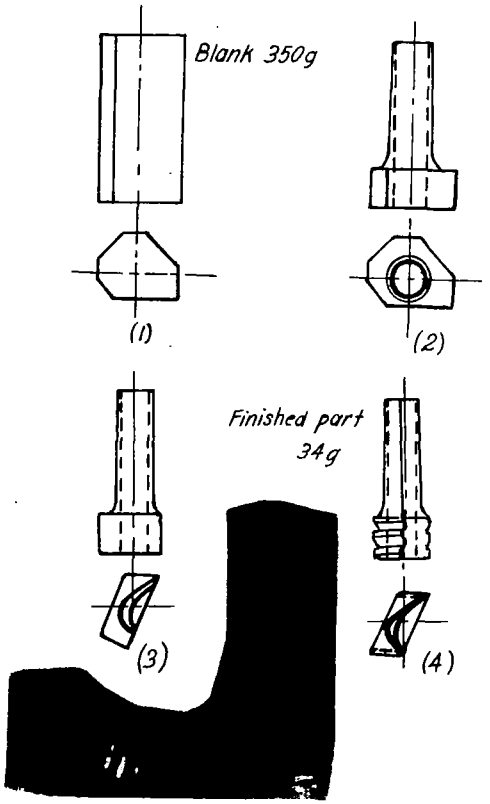

Figure 23.- Seamless hollow blade.

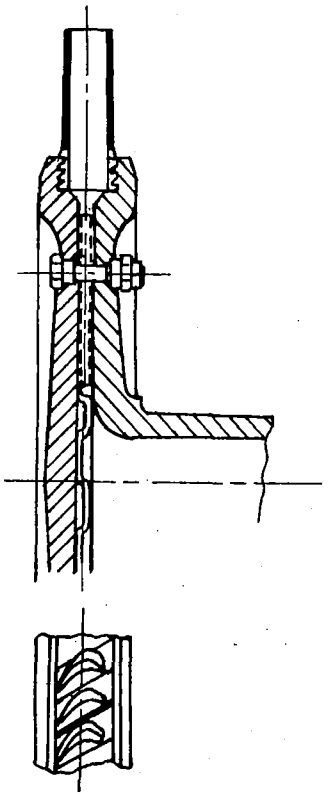

Figure 24.- Mounting of seamless hollow blade.

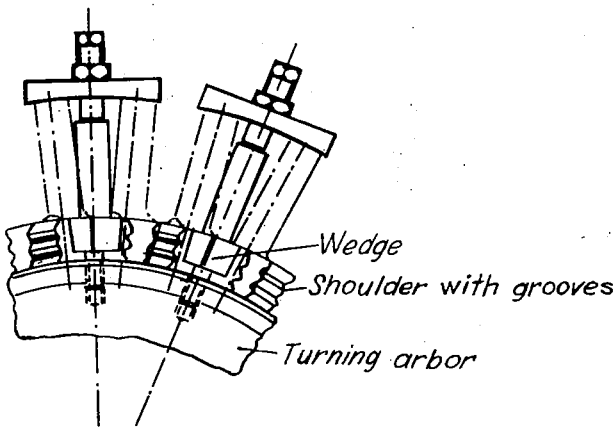

Figure 25.- Device for turning attachment grooves in blade root.

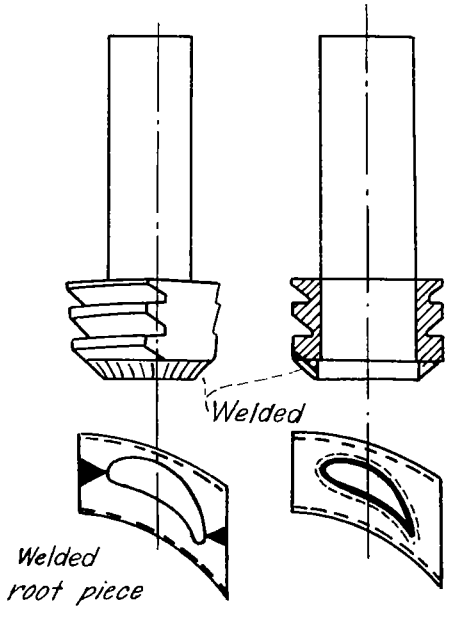

Figure 26.- Two-piece hollow blade.

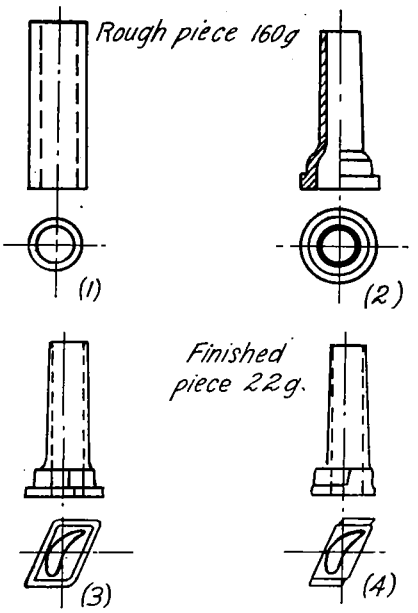

Figure 27.- Seamless blade made from tubing.

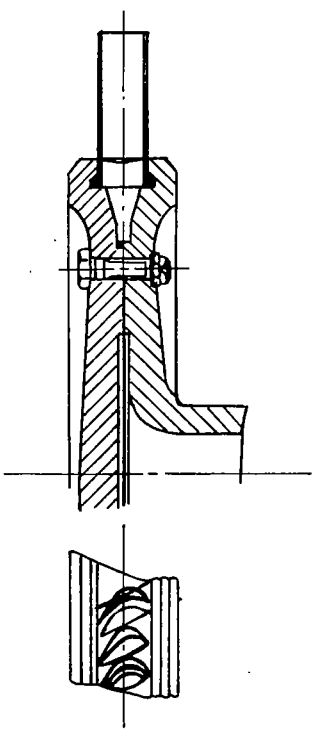

Figure 28.- Installation of seamless tubing hollow blade.

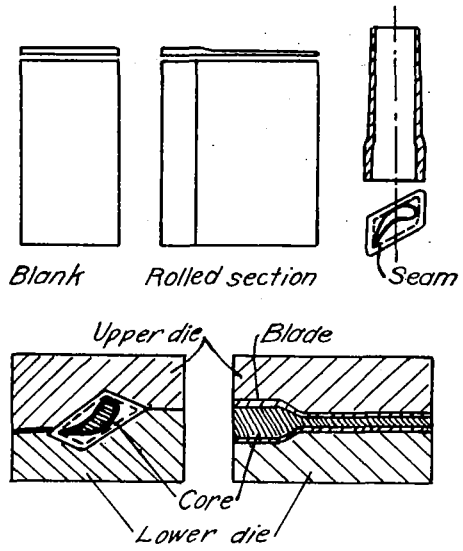

Figure 29.- Manufacture of hollow blade from sheet metal.

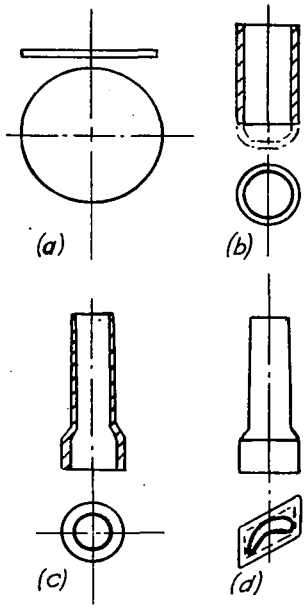

Figure 30.- Manufacture of box-root blade by drawing process.

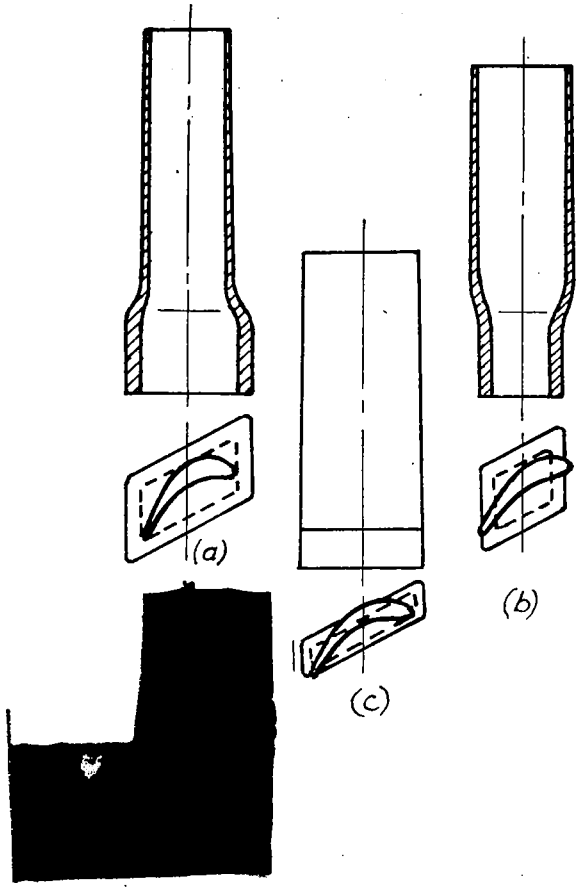

Figure 31.- Examples of blades with box-root.

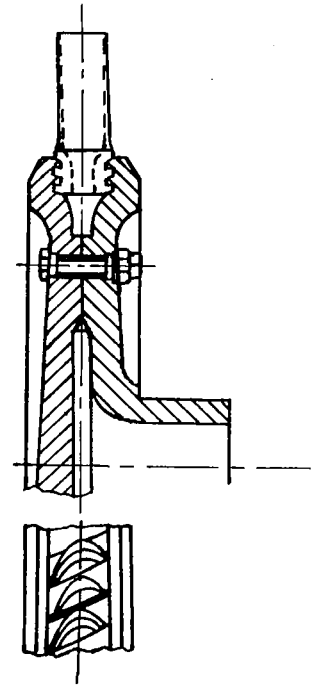

Figure 32.

Figure 33.

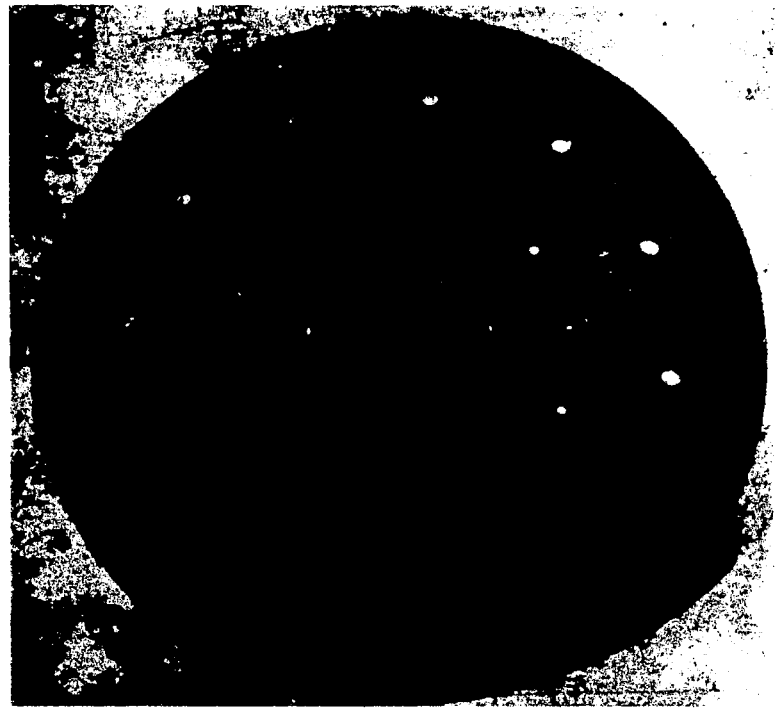

Figure 34.

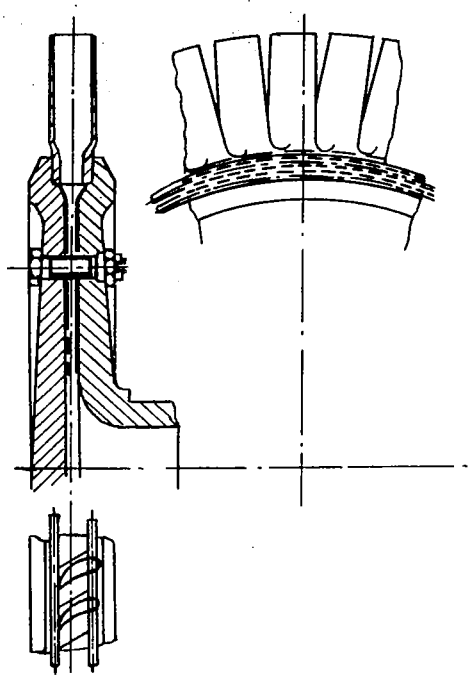

Figure 35.- Mounting of box-root blade by means of wire ring.

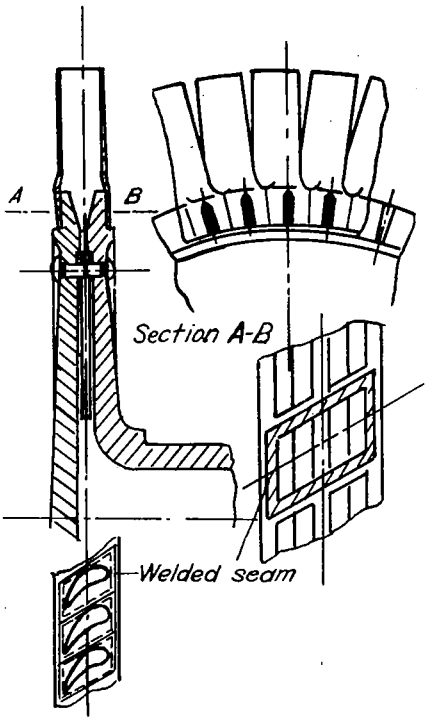

Figure 36.- Box-root blade mounted on wheel from the outside and welded.

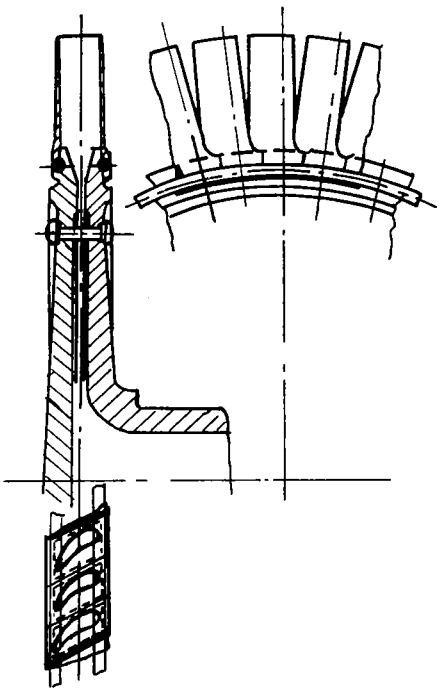

Figure 37.- Blade mounted from the outside - fastened by means of rings.

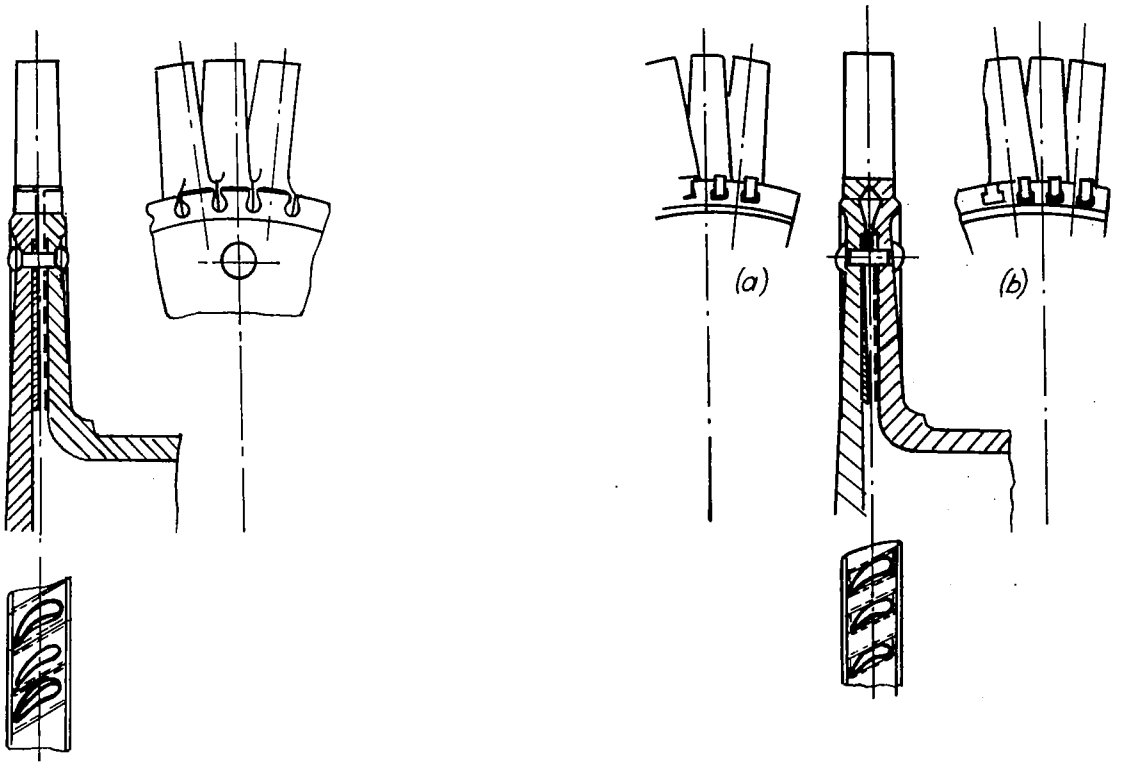

Figures 38 and 39.- Mounting of blade with small box-root in axial grooves over the circumference of the wheel.

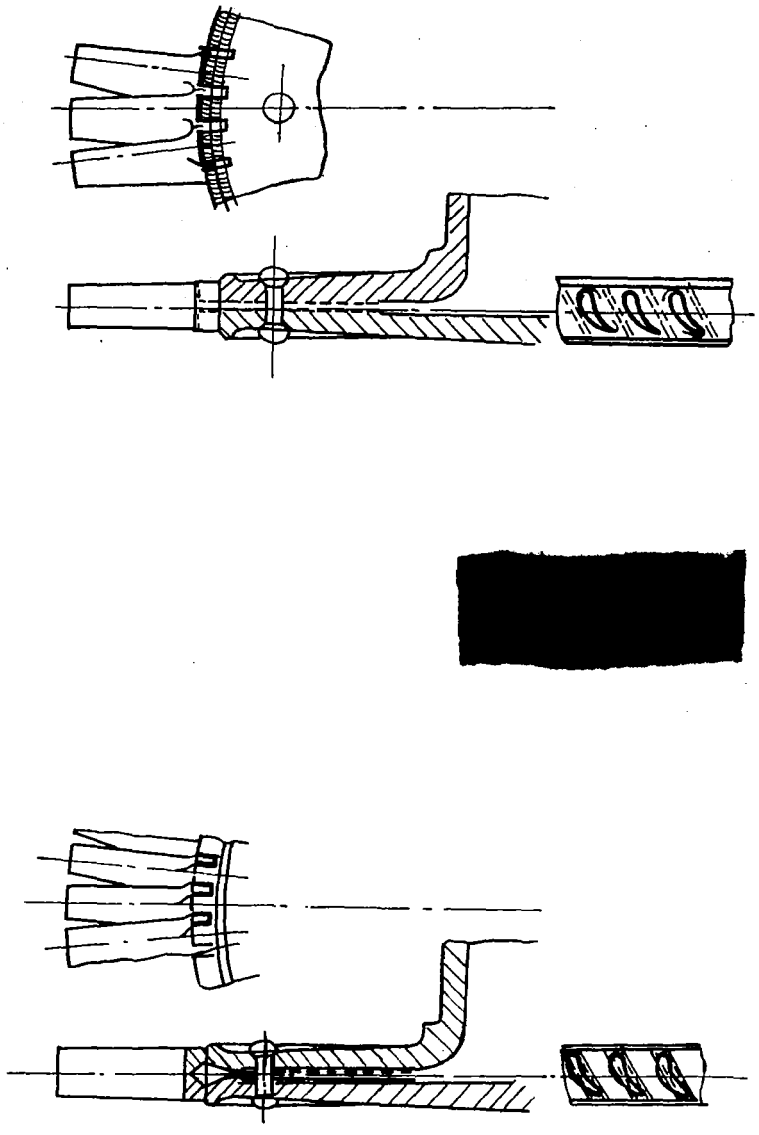

Figures 40, 41, and 42.- Attachment of the hollow blade in axial grooves.

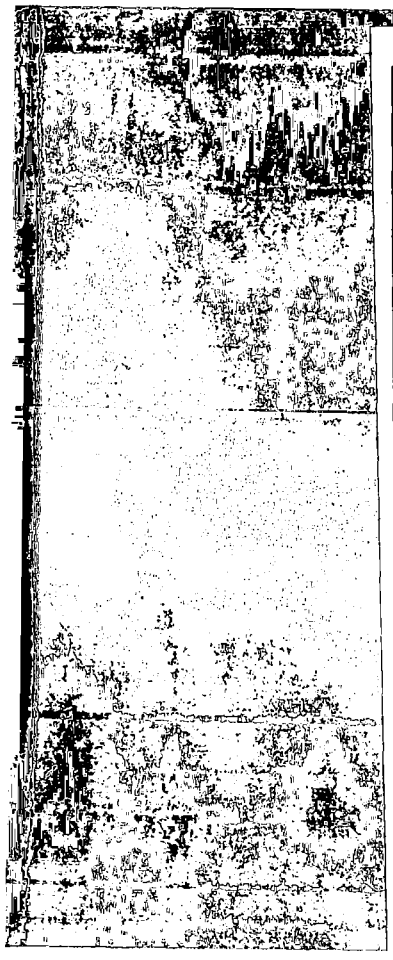

DO NOT REMOVE SLIP FROM MATERIAL

Delete your name from this slip when returning material to the library.

NAME	Date	MS
MARTHA MARIETTA	23 JAN	ILL

NASA Langley (Rev. May 1988) RIAD N-75